energies

MDPI

Article

Wireless Drone Charging Station Using Class-E Power Amplifier in Vertical Alignment and Lateral Misalignment Conditions

Aqeel Mahmood Jawad [1,2], Rosdiadee Nordin [1,*], Haider Mahmood Jawad [1,2], Sadik Kamel Gharghan [3], Asma' Abu-Samah [1], Mahmood Jawad Abu-Alshaeer [4] and Nor Fadzilah Abdullah [1]

1 Department of Electrical, Electronic and Systems Engineering, Faculty of Engineering and Built Environment, Universiti Kebangsaan Malaysia, Bangi 43600, Selangor, Malaysia; aqeel.jawad@ruc.edu.iq (A.M.J.); haider.jawad@ruc.edu.iq (H.M.J.); asma@ukm.edu.my (A.A.-S.); fadzilah.abdullah@ukm.edu.my (N.F.A.)
2 Department of Computer Technology Engineering, Al-Rafidain University College, Baghdad 10064, Iraq
3 Department of Medical Instrumentation Techniques Engineering, Electrical Engineering Technical College, Middle Technical University, Baghdad 10001, Iraq; sadik.gharghan@mtu.edu.iq
4 Department of Statistics, Al-Rafidain University College, Baghdad 10064, Iraq; dean@ruc.edu.iq
* Correspondence: adee@ukm.edu.my; Tel.: +603-8911-8402

Abstract: Recent major advancements in drone charging station design are related to the differences in coil design between the material (copper or aluminum) and inner thickness (diameter design) to address power transfer optimization and increased efficiency. The designs are normally challenged with reduced weight on the drone's side, which can lead to reduced payload or misalignment position issues between receiver and transmitter, limiting the performance of wireless charging. In this work, the coil combination was tested in vertical alignment from 2 cm to 50 cm, and in lateral misalignment positions that were stretched across 2, 5, 8, 10, and 15 cm ranges. Simulated and experimental results demonstrated improved transfer distances when the drone battery load was 100 Ω. With the proposed design, the vertical transfer power that was achieved was 21.12 W, 0.460 A, with 81.5% transfer efficiency, while the maximum lateral misalignment air gap that was achieved was 2 cm with 19.22 W and 74.15% efficiency. This study provides evidence that the developed circuit that is based on magnetic resonant coupling (MRC) is an effective technique towards improving power transfer efficiency across different remote and unmanned Internet of Things (IoT) applications, including drones for radiation monitoring and smart agriculture.

Keywords: drone battery life; energy efficiency; force-sensing resistor; multi-turn copper wire coil; lateral misalignment; power consumption; single tube loop aluminum coil; vertical alignment

Citation: Jawad, A.M.; Nordin, R.; Jawad, H.M.; Gharghan, S.K.; Abu-Samah, A.; Abu-Alshaeer, M.J.; Abdullah, N.F. Wireless Drone Charging Station Using Class-E Power Amplifier in Vertical Alignment and Lateral Misalignment Conditions. *Energies* **2022**, *15*, 1298. https://doi.org/10.3390/en15041298

Academic Editors: Charles Van Neste and Lei Zhao

Received: 7 December 2021
Accepted: 19 January 2022
Published: 11 February 2022

1. Introduction

As the need for charging electronic devices continues to increase, so does the demand for energy as a necessary component of our daily lives [1]. Wireless power transmission (WPT) comprises different technologies for the transmission of electromagnetic (EM) energy through physical matter and objects, such as, air, water, or walls [2]. Unlike traditional wire-based power transmission, WPT technology is not constrained by cables and does not produce electrical sparks, thus enabling high mobility charging [3]. Furthermore, damaged or loosened copper cables present a hazard when charging devices [4,5]. Therefore, wireless charging autonomy is the preferred method of energy pooling over short or medium ranges for devices, such as drones, after achieving close contact with a power source [6]. Drones or unmanned aerial vehicles (UAVs) generally operate on high-powered batteries, such as Li-po batteries, resulting in limited flight times and shorter distance deployments. The exhaustion of the power source onboard the aircraft is one of the main challenges of these systems in the fixed missions of any UAV [7]. Equipping drones with a larger battery unit

does not solve the problem as it increases the weight of the aircraft, thereby reducing the available weight for the payload, such as the coil, which is a critical element in WPT [8].

Secondly, a UAV or drone battery must often be charged for a long time. Therefore, highly efficient battery use during flight requires direct intervention from humans or the drone must be completely independent during direct charging [9]. However, wireless charging of the drone battery depends on the coil's design diameter, outer and inner coil, and the number of turns to increase the transfer power efficiency and distance between the two coils. The imbalance in lateral misalignment distance between two coils while charging is a permanent electrical engineering problem that remains a challenge [10]. Therefore, this problem has prompted the need for continuous verification because the two coils are usually not perfectly aligned due to differences in the coupling factors and the wrong hovering position of the drone. Moreover, these differences can decrease the transfer distance and power transfer efficiency of the receiving coil, causing fluctuations during the charging process [11]. Therefore, improving the energy transfer efficiency and transfer distance in several directions is crucial to achieve energy transmission with high efficiency. Generally, to alleviate this problem, the diameter of the primary winding must be greater than the diameter of the secondary winding and equal to twice the distance between the two windings [12], or a group of several fixed primary windings must be used to charge a single winding [13].

Some researchers have studied the problems of limited battery life, long charging times, short distances, precision requirements when smart devices use a transmitter pad with the axial alignment distance and lateral misalignment in different directions, and low transfer power efficiency for long distances. The coil dimensions are defined correctly when the axes of the z parameters of the coupled coils coincide at an axially aligned distance perfectly [14]. The rotation of the plane containing one coil from a pair of coupled coils without a change in the coil alignment results in planar rotation [15]. Range variations arise from changes in the distance between a pair of coupled coils. The vertical alignment could manifest in two forms: angular or lateral misalignment. These alterations in configuration may occur individually or could appear together at varying degrees in a coupled interaction between the transmitter and the receiver coils.

Drones are expected to be the strength of smart flying as they could act as the first respondent to any emergency that may arise. However, they have a huge limitation of having very low-power densities, an inability to sustain longer flight times, and hovering in the wrong directions that cause loss of power [16]. To optimize energy transfer performance, the misalignment transmission distance between the transmitter and receiver coils is the main limitation of magnetic resonator coupling (MRC) methods, which are sensitive to transmitting and receiving coil alignment. However, this is limited by each of the coils' diameters (large or small), the line spacing of each coil, and the distance between the transmitter and receiver coils [17]. Researchers have been attempting to reduce misalignment using two major approaches [18]. The first approach is the auto-alignment of the two coils by either the movement of the transmitter or receiver coil, and the second is through electrical manipulation, such as resonance or modifying compensation topologies. Regardless, major challenges in the adoption of WPT technology still exists due to the types of power amplifiers that are available for far-field applications.

Two methods can be implemented to improve payload due to charging purposes and the misalignment challenges. First, the battery of the transmitter circuit can be automatically charged after the drone lands at the base station. However, this method is still unfeasible due to the inaccuracy of landing positions. Second, the battery of the transmitter circuit can be charged by the battery of the receiver coils of the drone by using a class E power amplifier (PA). In addition, a spiral coil platform is used for the force-sensing resistor (FSR) as an ON/OFF switch for drone landing that gives higher accuracy during battery charging of the coil receiver.

The two techniques that can be implemented for the drone charging station were considered as solutions in this paper. The first method optimizes the weight of a coil

against maximum transfer efficiency and distance by testing several coils parameters in a simulation and selecting the best material such as aluminum or copper. The second method is to use an electrical connection (such as a Class E PAs) between the drone coil receiver and the transmitter station coil.

This work aims to solve the misalignment's tolerance by simulating and designing a suitable coil for the platform station between the transmitter and receiver side at various distances. In addition, our work proposed using FSR as the first solution to know the landing position of a drone on the platform. Because a drone cannot hover in a static position and can fluctuate in angular and planar misalignment situations which cause difficulty in modelling, this study concentrated on two types of misalignments, i.e., vertical misalignment and lateral misalignment (horizontal). This is most common in drones that are used in applications such as radiation monitoring and smart agriculture. The drone is controlled remotely in a fixed straight path and air impedes diagonal movement between the wings.

This study proposes a drone charging platform based on a new WPT design and analysis method under vertical and misalignment conditions. The study considers the misalignment between the transmitter and receiver coils focusing on transfer power, efficiency, and distance. The WPT system was designed, simulated, implemented, and tested considering the suitable weight of the landed drone and by maintaining drone hovering conditions.

The design was obtained after different simulations and validated with an experimental laboratory test. The main focuses regarding WPT were the transfer coupling coefficient, quality factor, mutual inductance, transfer power, coil design, and to some extent, the transfer efficiency increases as described in [9]. Several articles have discussed the major concerns about recharging the battery using the WPT-based misalignment coil approach [10,19–21], and they are highlighted in the next section.

2. Related Works

Transfer power and efficiency are common problems in designing WPT as both result in decreased system performance. Misalignment between the transmitter and receiver coils of a WPT system for charging a drone battery has posed an additional challenge, especially in transferring higher power at high efficiencies, which has limited the potential use of WPT for future applications such as in the IoT [22]. Therefore, several studies have been directed in this area in recent years. However, the misalignment between coils in WPT still poses a challenge. Although many researchers have conducted experiments, and extensive efforts have been made on the development of near-field (NF) WPT techniques (i.e., IC and MRC) and have been presented, several practical challenges have yet to be fully resolved. These include coil orientation, air gap, transfer power, transfer efficiency, operating frequency, misalignment positions, coil weight, coil size, and electromagnetic radiation interference, especially in high frequency applications with RF components. The main advantages of all onboard components are their lightweight and compact designs.

Several researchers have reviewed alignment and misalignment conditions in terms of distances and angles and found several solutions such as the minimization of variations in the perpendicular component of the magnetic field [10], a solution to the inverse field problem [19], tunability of the impedance network [21] and repressing the increase in mutual inductance [23]. These solutions can increase transfer efficiency, power, and distance for this type of misalignment solution [8,14,24].

Campi et al. [25] designed a primary coil (copper Litz wire on the receiver and tube coils on the transmitter) to withstand severe coil misalignment conditions; the landing gear of the secondary coil with a suitably formed aluminum tube has a minimal effect on the drone's (DJI F550 with five motors) aerodynamics, coupled with the additional weight (78 g) of the platform station. According to the results, the proposed system reduced the electrical loss and maintained good mechanical properties by assuming a different size of landing gear (e.g., the landing point height) and a frequency of 300 kHz with a maximum

power of 70 W. These results demonstrated that in the design circuit, series–series topology (S–S) is better than series–parallel (S–P) according to the number of turns of the primary coil, which range from 1 to 10. They also tested several load resistances (R_L) from 1 to 20 Ω with 90% to 95% transfer efficiency between the calculated and measured misalignment ranges (from 5 to 30 cm) between the x-axis and y-axis. In this work, there is a small coil design on the drone and a large tube coil with a 10-turn coil on the platform station, which is a limitation of the work as the system loses more power.

Lan et al. [26] presented a Class EF PA inverter and Class D rectifier based on a high-frequency MRC system built with lightweight copper pipe air-core coils at both ends and lightweight electronics on the receiver side. The designed WPT charging platform is circular with a 1m diameter, thus allowing for the lateral misalignment of up to 250 mm with a transfer efficiency of 70% and a frequency of 6.78 MHz. The DJI Matrice 100 quadcopter drones were supplied with 22.2 V and 4500 mAh with a Lithium-Polymer (Li-Po) battery for WPT, which was designed to charge the same battery when using wire. The designed coil (inner: 350 mm and outer: 40 mm) was built with a box (platform) with a two-turn square shape for an increased Q-factor and inductance of 1143 and 1.13 µH, respectively, with a 140 mm transfer distance capacity. The drone landed on the charging pad nine times successfully.

Yusmarnita et al. [27] proposed a Class E PA by studying the effect of switching and performance analysis behaviors at a frequency of 1 MHz. They designed an electronic circuit (using a Proteus simulation electronic circuit) based on Class E PAs, then analyzed and compared the measured, theoretical and simulated results. The electronic circuit design consists of the resistance load network and a single transistor operated as a switch at the carrier frequency of the output signal. The simulation experiment achieved a power input and output of 9.84 and 8.62 W, respectively, with an efficiency of 87.56%. The experimental result achieved 98% transfer efficiency with 9.60 and 9.45 W power input and output values. Finally, the theoretical calculation reached 10 W of input and output power, with a transfer efficiency of 100%. The operating frequency of the proposed system was equal to 1 MHz. The switch control signal type was IRF510 MOSFET, which used a PIC16877A microcontroller, and the results indicated that the zero-voltage switching (ZVS) condition could be completed effectively.

Wang and Song, et al. [28] presented a circuit based on Class E PAs using a ZVS oscillator. The theoretical calculation and simulation of MRC WPT system parameters were investigated. They achieved high power–delivery efficiency and low current according to an analysis of the load current waveform (0.156 A) and voltage (28.2 V). In their paper, they introduced theoretical and simulation results without the designed coil. Their calculation results showed improvement in the transfer efficiency with low current and a high voltage of 29.34 V. However, the comparison between the calculation and simulation results was inconsistent with the analyzed theoretical results.

Kang et al. [29] proposed and analyzed the effect of the misalignment of resonators based on an MRC wireless power-charging system that used a slit ground resonator on a laptop computer with a dimension of 24.5 cm × 39 cm. The proposed system was tested in correct alignment and misalignment conditions. The design achieved good results when used in alignment conditions. However, the transfer efficiency decreased by 45% when there was a misalignment between the movable receiver and the transmitter. The tube coils were designed for the transmitter (one turn as a square) and receiver (five turns in a circlular shape), resulting in the mutual inductance of 0.905 µH at 100 mm when increasing the diameter to 600 mm for both coils. The results improved the mutual inductance and k in lateral misalignment distance. This is useful only for charging laptops on a table when increasing the diameter of coils with a transfer efficiency of 55% at 200 mm. Note that by designing the big rectangular coil geometry, such as its width, dimension, and number of turns on the transmitter side and the circular coil on the receiver side at the center, the misalignment tolerance between a transmitter and receiver coil can be solved.

Rybicki et al. [30] presented a prototype of an MRC system in the design of a Class E PA, which was selected due to its ability to achieve highly efficient DC–AC conversion. However, the serial to parallel (S–P) connection of resonance capacitors was intended to operate at 1 MHz at high frequency. The selection of the rectifier parameters allowed operation at a high efficiency (80%) and with a transfer distance of 7.5 cm, with a k equal to 0.196 of RLC impedance through the simulation and analysis of the matching circuit coil design.

The WPT system suffers from reduced transmission performance during energy transmission due to the mismatch between the cores of the two coils (transmitter and receiver). Many types of alignment configuration exist between coils, such as vertical variation, planar, angular, lateral (horizontal), planar and horizontal, and angular horizontal [31]. All alignments have different directions and applications. Thus, the basic parameters, such as mutual inductance, efficiency, and output power, vary during experiments [32]. Rohan et al. [33] used an intelligent automatic alignment algorithm based on the hill climb algorithm to control misaligned coupling between coils. A control unit was suggested and executed to measure the terminal voltage of each transmission coil and align the midpoint of the transmiting and receiving coil.

In most recent studies, several attempts using the multi-loop topology in impedance matching have made sure that the MRC state, even with a differing distance between the transmitting and receiving coils, reduced the variation of the input impedance [34]. The general technique [35] developed by Massachusetts Institute of Technology (MIT) researchers is a highly resonant magnetic WPT, which reduces the misalignment problem to a certain extent for 2 m of transfer distance. WPT is limited by three factors: (1) Efficient and long-distance power transfer; (2) The International Commission on Non-Ionizing Radiation Protection (ICNIRP) established limits on the strength, frequency, and other factors of electromagnetic radiations and fields used in wireless applications; and (3) the IEEE and ICNIRP established electromagnetic radiation limits, which may make designing a system difficult. The lateral misalignment distance depends on the efficiency and air gap of various factors, such as coil directions, alignment, frequency, and coil design between the transmitter and receiver coils of the WPT system.

This paper aims to address two problems that were not tackled in the previous studies. The first was the receiver coil's payload minimization, which can be solved by choosing lighter materials (e.g., aluminum) and testing the coil design by simulation. The second problem is the issue of low transfer power in misalignment conditions. We propose to solve this problem by improving the design of a Class E PA at the transmitter circuit.

3. WPT System Design

The following subsections explain the mathematical and simulatory foundations of the WPT and the design of the proposed multi-tube spiral copper coil (MTSCC) at the transmitter circuit, and single-tube loop aluminum coil (STLAC) at the receiver with the related parameters. In this work, the design of the proposed basic WPT system has been revised using simulatory and experimental approaches with different aligned and misaligned coils.

3.1. WPT Simulation Models

The resonant frequency (f_r) for the input and the output circuit is proposed to be 1 MHz. Given the chosen value, the capacitance of transmitter (C_S) and receiver (C_R), and the inductance of the transmitter (L_S) and receiver (L_r) coils can be computed with the following Equation (1) [36]:

$$f_r = \frac{1}{2\pi\sqrt{L_s C_s}} = \frac{1}{2\pi\sqrt{L_r C_R}} \quad (1)$$

Re ($Z_{1,1}$), *Re* ($Z_{2,2}$), *Im* ($Z_{1,1}$), and *Im* ($Z_{2,2}$) represent the real and imaginary parts of the *Z*-parameters of both the transmitter and receiver. The quality factors of the transmitter (Q_1) and receiver (Q_2) coils are calculated from Equations (2) and (3) [37]:

$$Q_1 = \frac{Im\ (Z_{1,1})}{Re\ (Z_{1,1})} \tag{2}$$

$$Q_2 = \frac{Im\ (Z_{2,2})}{Re\ (Z_{2,2})} \tag{3}$$

The *Im* of both the transmitter and receiver coils are given as *Im* ($Z_{1,1}$) and *Im* ($Z_{2,2}$), respectively, while the coil L_S and L_r can be calculated as shown in Equations (4) and (5) [37]:

$$L_S = \frac{Im\ (Z_{1,1})}{2\pi f} \tag{4}$$

$$L_r = \frac{Im\ (Z_{2,2})}{2\pi f} \tag{5}$$

The other component, the mutual inductance (M) between transmitter and receiver coils can be obtained from a simulation of the *Z*-parameter as in Equation (6), and the coupling coefficient (k) is calculated from Equation (7):

$$M = \frac{Im\ (Z_{2,1})}{2\pi f} \tag{6}$$

$$k = \sqrt{\frac{Im\ (Z_{1,2})\ Im\ (Z_{2,1})}{Im\ (Z_{1,1})\ Im\ (Z_{2,2})}} \tag{7}$$

The maximum WPT efficiency (Max.WPTE) is represented by ($\eta_{\max}$) as in Equation (8) [38]:

$$\eta_{\max} = \frac{k^2 Q_1 Q_2}{\left(1 + \sqrt{1 + k^2 Q_1 Q_2}\right)^2} \times 100\% \tag{8}$$

The overall power transmission efficiency between the transmitter and receiver is often denoted by the transfer efficiency link (η_{link}), which will be investigated throughout the rest of this paper. Based on the η_{link} optimum load resistance level chosen according to Equation (9) [14], the load quality factor (Q_L) of the WPT system in simulation can be obtained from the following equation:

$$\eta_{link} = \frac{k^2 Q_1 Q_2^2}{(Q_L + Q_2)\left(\frac{Q_2}{Q_L} + k^2 Q_1 Q_2 + 1\right)} \times 100\% \tag{9}$$

The load resistance (R_L) can be obtained through Equation (10),

$$Q_L = 2\pi f \times C_{S\ and\ R} \times R_L \tag{10}$$

where the parasitic capacitance of transmitter (C_S) and receiver (C_R) coils are presented in Equations (11) and (12) [39].

$$C_S = \frac{1}{4 \times \pi^2 f^2 \times L_S} \tag{11}$$

$$C_R = \frac{1}{4 \times \pi^2 f^2 \times L_r} \tag{12}$$

Using ANSYS HFSS V15.03 solver simulator software [40], STLAC and MTSCC designs can be easily calculated using *Z*-parameters. The other method for improving the Q_L when lowering the real part of the *Z*-parameters was achieved using a high line-space (referring

to the distance between each number of turns) for the resonant tube coils. However, high line-space coils are heavy, and the amount of weight a UAV can carry is limited.

In this paper, the design uses a heavy multi-tube spiral copper coil on the station's pad for the transmitter and a low weight single-tube aluminum coil for the receiver to be carried on the drone to reduce the payload. Using a Class E PA, an operating frequency of 1 MHz was adopted to design the two types of misalignment cases (i.e., vertical alignment and lateral misalignment) in simulated and measured transmitter circuit designs.

3.2. WPT Coil Mathematical Model

The first step of the theoretical WPT design is the self-inductance for both the receiver's STLAC and the transmitter's MTSCC as shown in Equation (13) [4]:

$$L = \mu_o \, \mu_r R \, {N_T}^2 \left(\ln \frac{8R}{a_i} - 1.75 \right) \tag{13}$$

where L is the inductance of the coil (μH), μ_o is the vacuum permeability ($4\pi \times 10^{-7}$ H/m), mu_r = 1 is the relative permeability of the conductor, R is the loop radius of the coil, N_T is the number of coils turns, and a_i is the radius of the wire or tube cross-section. Moreover, additional values were calculated when using tube and wire coils. Equation (14) must be calculated to identify the factor parameter (φ), outer diameter of the coil (d_{out}/mm), inner diameter (d_{in}) and to find the most suitable number of turns for each coil [41]; it ranges from 0 to 1.

$$\varphi = \frac{d_{out} - d_{in}}{d_{out} + d_{in}} \tag{14}$$

Using the inductance L of the tube coil as given in Equation (15), the same parameters were used for the copper coil to find the average diameter of the coil (d_{avg}) and the d_{out} and d_{in} values [42]:

$$d_{avg} = \frac{d_{out} + d_{in}}{2} \tag{15}$$

where N_T is the number of turns that can be calculated from Equation (16).

$$N_T = \frac{d_{out}}{S + W} \times \frac{\varphi}{1 + \varphi} \tag{16}$$

The coil line width (W) can be calculated from the minor radius of each coil and S, which represents radius change per turn for all types of coil design (i.e., STLAC and MTSCC). Utilizing Equation (17), d_{out} and d_{in} can be calculated based on the N_T, S, and W of the coil conductor as:

$$d_{out} = d_{in} + (2 \, N_T + 1)W + (2N_T - 1) \, S \tag{17}$$

Reduced distance separation between coil turns (S) improves the magnetic coupling of the coil windings and reduces the area needed for the platform station. A large spacing is preferred to reduce the parasitic loss (C_L) and the parasitic capacitance (C_p) between line traces of the coil turns. As it exhibits a maximum error of 13% (2 mm/W = 15 mm) for $S \leq 15$ W, designers must carefully select the line space/line width (S/W) ratio. Typically, spiral tube inductor coils are built with ratios where $S \leq W$ [43].

Equation (18) is used to calculate the Q_1 and Q_2:

$$Q_{total} = Q_1 = Q_2 = \frac{1}{R}\sqrt{\frac{L}{C}} \tag{18}$$

where R is the resistance of the standard coil (Ω), which is equal to 50 Ω according to the Voltage Standing Wave Ratio (VSWR), and L is the same term that was calculated in Equation (13). The quality factor can be increased in two ways, by either lowering the capacitance or the resistance as shown in the previous (Equations (3) and (4)). Capacitance

is quickly decreased by either pairing a capacitor in series or by using new capacitors with a lower value. The real effect of a low capacitance is a high resonant frequency, as shown in Equation (5); this limits significant currents from voltages that have less time to overcome magnetic moment, which is the magnetic strength and orientation of a magnet or other object that produces a magnetic field, based on the definition given by Gauss or Tesla [44].

In the near field, coil geometries aiming to optimize wireless link efficiency are affected by a set of parameters, such as a coil's *Q-factor* and *k*, which are limited by other factors related to the fabrication technology. As the priority is to define the overall coil size constraints, the design will then indicate the minimum size features that will provide an acceptable manufacturing yield. The typical size of drone coils used is 400×400 mm^2 and the coupling distance between the coils is 20 mm (near-field distance). As the transmitter of the coil is placed in the platform station, there is greater flexibility regarding the amount of turns, weight, and size.

Other important parameters that affect the coil size are the operating frequency (f_o) and the load resistance R_L. The fabrication process favors the minimum feature sizes, such as the minimum line width $W_{\min}$, minimum line spacing ($S_{\min}$), minimum thickness, and the substrate and conductor material properties. The operating frequency was designated as 1MHz. In this paper, the *Q-factor* and *k* are the main parameters considered to affect the power transmission efficiency of the WPT link. These parameters are particularly impacted by the platform station's geometric variables, such as the coil's outer diameter (d_{out}), spacing between the conductors (S), and the width of conductors (W) in the primary and secondary coils. Accordingly, these variables were selected for optimization to obtain the optimal *Q-factor*, *k*, and from that, the most appropriate PTE. Therefore, it is not possible to use the platform station (transmitter coil) to transfer far-field power, which is related to the design coil structure. In addition, moisture, heat, etc. also affected the transfer of energy between coils.

4. Challenges and Limitations of Misalignment Conditions for Drone Charging Platform

The WPT system suffers from reduced transmission performance during energy transmission due to the mismatch between the cores of the transmitter and receiver coils. This misalignment condition can be further classified into many types based on their simultaneous position. Figure 1 illustrates the various types of configuration, such as (a) vertical, (b) planar, (c) lateral, and (d) angular–vertical [31]. Planar and angular–vertical configurations are more difficult to model for drone applications because drones are unable to hover in a static position and keep fluctuating. These configurations are more relevant for applications, such as electric vehicles, implantable medical devices, laptops, and mobile devices. Cai, et al. [45] introduced a matrix of multiple transmitter coils for charging drones and used a current sensor (an STM32 controller) to detect misalignment.

Drones are expected to be the pinnacle of smart flying as they may act as the first respondents to any emergency that may arise. However, even without hovering in the wrong directions, they have a low-power density. Thus, a long sustained flight is impossible [16]. To optimize energy transfer performance, the misalignment transmission distance between the transmitter and receiver coils is the main limitation of MRC methods, which are sensitive to transmitting and receiving coil alignment. However, this is limited by the diameter (large or small), N_T, line spacing of each coil, and distance between the transmitter and receiver coils [17]. Researchers have been attempting to reduce misalignment using two major approaches [18]. The first approach is the auto-alignment of the two coils either by the transmitter or receiver coil movement, and the second is through electrical manipulation, such as resonance or modifying compensation topologies. Regardless, major challenges in the adoption of WPT technology still exist.

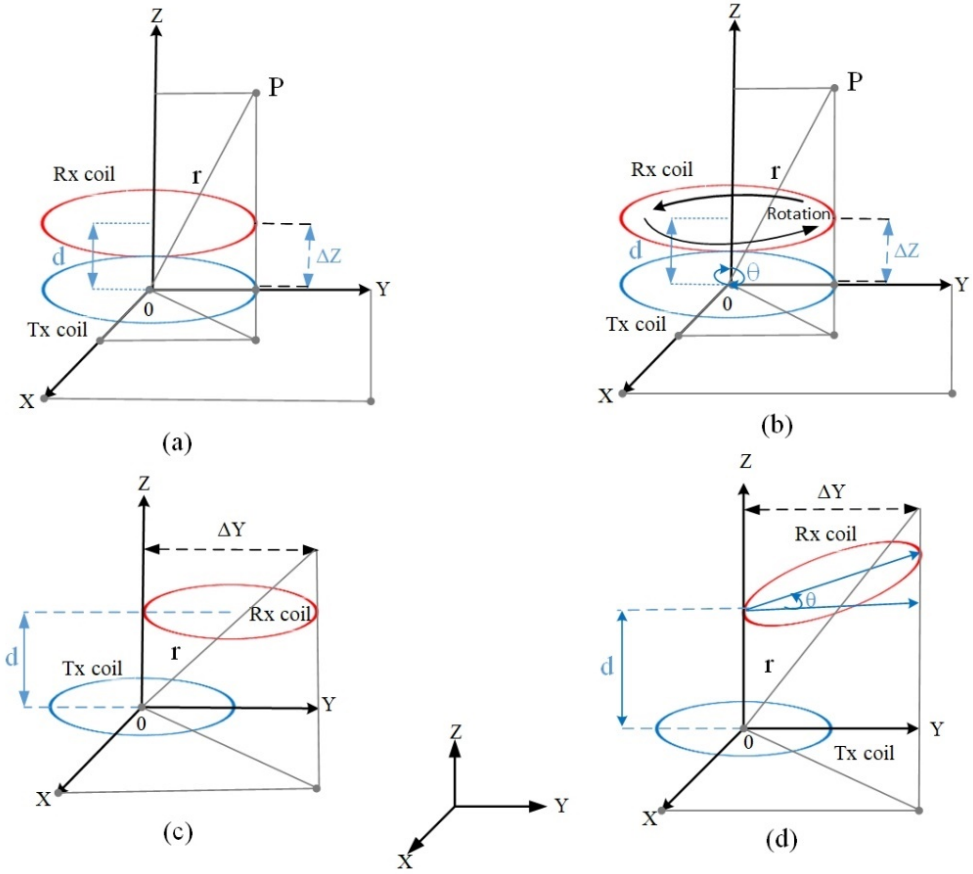

Figure 1. Schematics of circular coils for analyzed variations: (**a**) ideal alignment (vertical variation); (**b**) planar variation; (**c**) lateral misalignment; and (**d**) angular in lateral misalignment.

IC and MRC methods have the main advantages of high-power and long-distance transmission through different power amplifier types of far near field applications. However, the IC and MRC systems must deal with the inevitable key technical problem, which is the extremely loosely coupled effect between the transmitter and receiver coils. This corresponds to the measurement results found by [46], where k was mostly found to be much less than 0.01 within transmission distances of between 2 m and 12 m. Their experimental model can provide 10.3 W of power at up to 7 m distance, at a frequency of 20 kHz using dipole-coil-based IPT [47]. Therefore, the transmission air gap difference is another key technical concern for MRC systems because of the resonant frequency.

In other studies, several attempts using the multi-loop topology in impedance matching have been made to ensure the MRC state, even with a differing distance between the transmitting and receiving coils, to reduce the input impedance variation [34]. The technique developed by MIT researchers is a method of highly resonant magnetic WPT which reduces the misalignment problem to a certain extent for a 2 m transfer distance [35].

5. WPT Coil Design Simulation

This paper considers two misalignment methods for improving the NF-WPT between designed coils, i.e., the vertical and lateral configurations with different coil positioning variations. The Equations (1)–(9) were employed in the simulation phase to calculate L, Q, M, k, $\eta_{\max}$, and η_{link} of the improved coil, and to analyze the impact of transfer distance. Figure 2a,b illustrate the new design of receiver and transmitter coils, respectively, for charging the drone's battery. The receiver coil's d_{out}, was 420 mm with one turn, while the outer transmitter coil's d_{out}, was 418 mm. The transmitter coil has six turns and the internal dimension was 260 mm. The measured weights of the aluminum receiver and copper transmitter coils were 10.5 and 2000 g, respectively. Simulations to investigate transfer

distance and WPT efficiency for both misaligned configurations were done using ANSYS HFSS V15.03 software [48] with the following details.

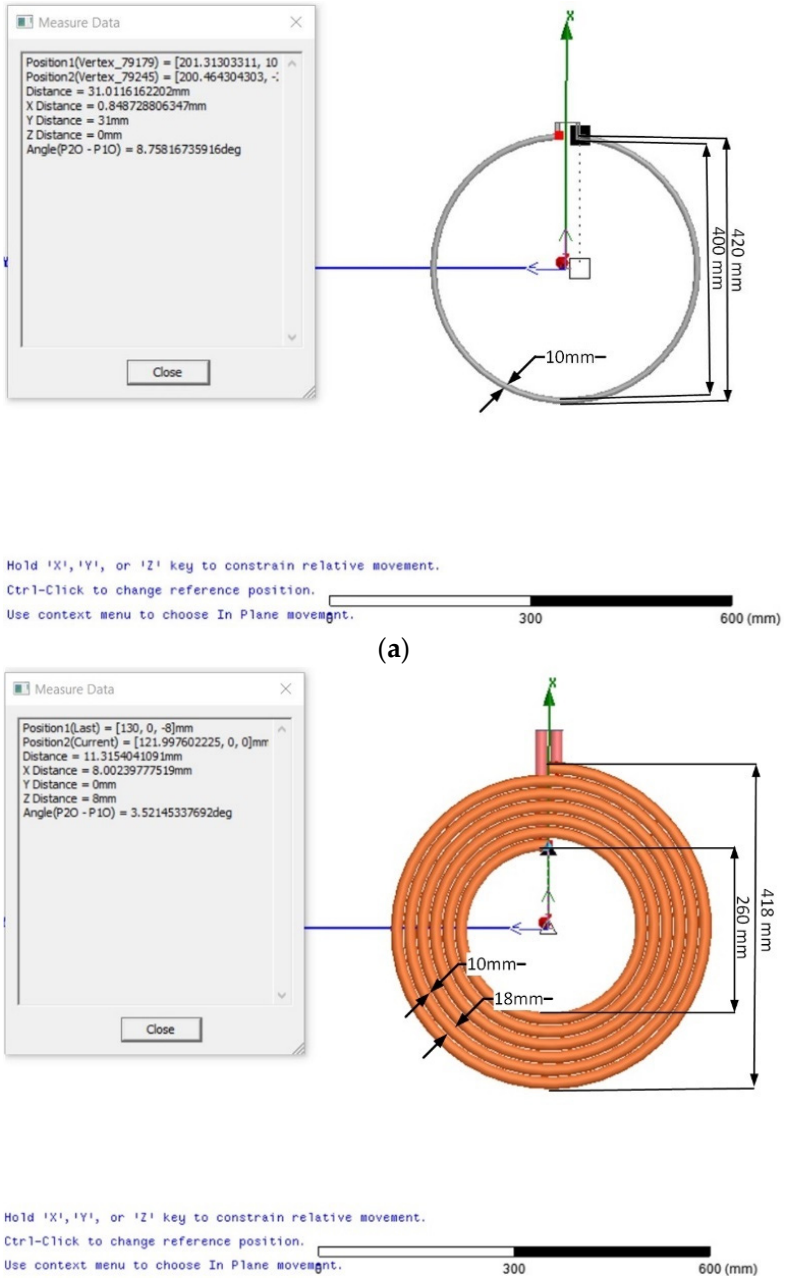

Figure 2. Designed coils to charge the drone's battery: (**a**) receiver coil, STLAC; and (**b**) transmitter coil, MTSCC.

5.1. Vertical Alignment

Figure 3 shows the HFSS simulator set up for the transmitter and receiver coils aligned to the *z*-axis test. Upon completing the drone's mission, and landing on the platform, the FSR sensor will check the drone's weight and the distance to the receiver coil to start charging the battery. The *x*-axis/vertical design approach first involves investigating drone charging in vertical alignment over several distances. In the simulation, seven transfer distances (2, 5, 10, 20, 30, 40, and 50 cm) of MRC-WPT were tested. The distance (X cm) with the best simulation results was then used in the misalignment simulation.

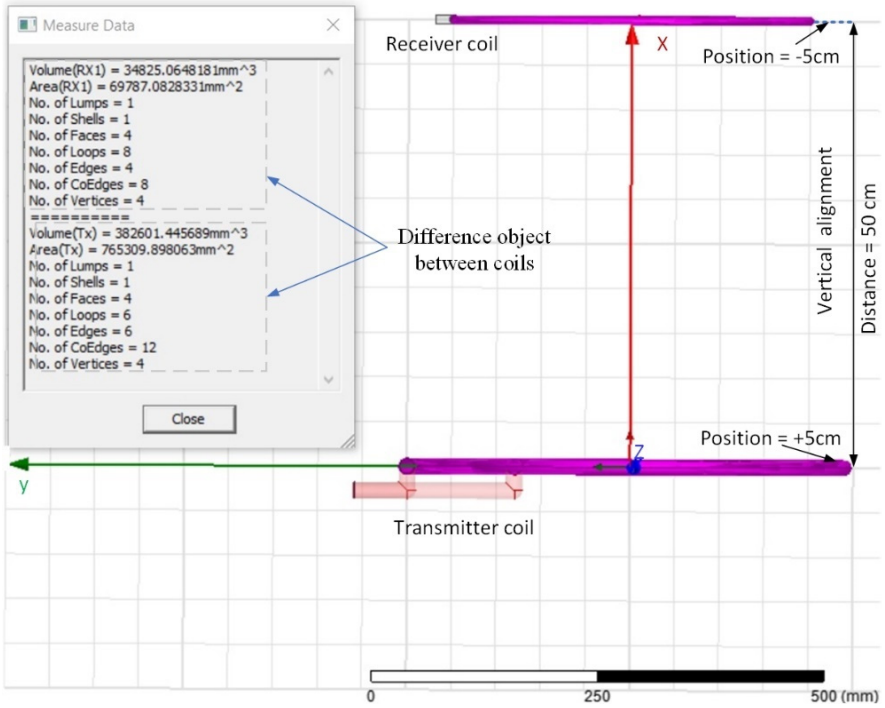

Figure 3. Alignment distance with *x*-axis at 2, 5, 10, 20, 30, 40, and 50 cm.

5.2. Lateral Misalignment

The second test for lateral misalignment involves the manipulation of the drone coil in the *y*-axis. In the HFSS simulator, the transmitter coil was fixed to the platform station and the *z*-axis was fixed at X cm (2 cm in our case). Meanwhile, the *y*-axis of the receiver coil, mounted on the drone, was moved through five steps of lateral misalignment distances (2, 5, 8, 10, and 15 cm), as shown in Figure 4. However, when a drone is hovering, especially before landing, another type of misalignment will appear and be regarded as secondary lateral misalignment. This misalignment type is also considered and analyzed in this paper. The 15 cm maximum range of drones in lateral misalignment between the receiver coil and platform station is a sufficient range for drone testing in the scope of this work.

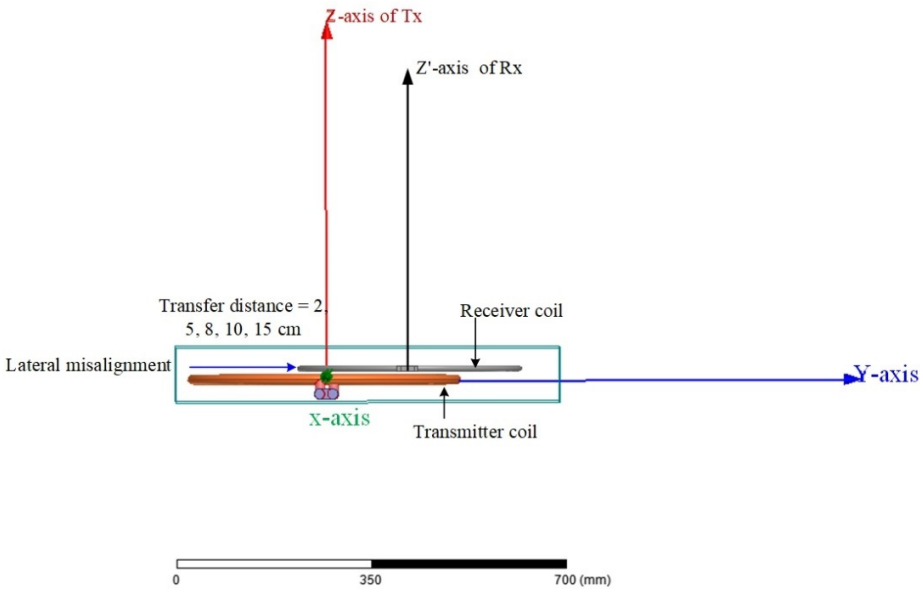

Figure 4. Lateral misalignment distance with the *y*-axis of lateral misalignment (drone landing) at 2, 5, 8, 10, and 15 cm.

6. Experimental Configuration of an MRC Misalignment Coil

The WPT system is intended for charging drones in various unmanned and remote applications such as remote monitoring. The WPT circuit considers the S–P topology connection of a 1 MHz resonance frequency. This approach uses coil structures, such as d_{out} and d_{in} to solve misalignment conditions. The MRC of the STLAC (receiver) and MTSCC (transmitter) coil types have been suggested to generate strong magnetic field leakage. Thus, a laboratory test on the MRC hardware design was conducted to validate the transfer distance and efficiency between the transmitter and receiver coils, using the highest performing coil design obtained from the simulation.

First, copper and aluminum loops of 420 mm (d_{out}) were used to design one turn. The inner coil diameter (d_{in}) was 400 mm, and a line distance width of 10 mm was used. The receiver coils were mounted on the wooden pad for laboratory testing. A circle of d_{out} = 418 mm and d_{in} = 260 mm was chosen to be identical to the asymptotic diameter of the transmitter coil. Then, a circular frame was constructed to design the transmitter coil and make the copper into a circular shape, as shown in Figure 5a. As mentioned previously, the circular shape promotes increased transfer efficiency by providing a more enclosed space (area) for a given distance (perimeter) than a square. The aluminum coil was chosen for the STLAC to ensure the lightweight of the receiver coil and maximum transfer power.

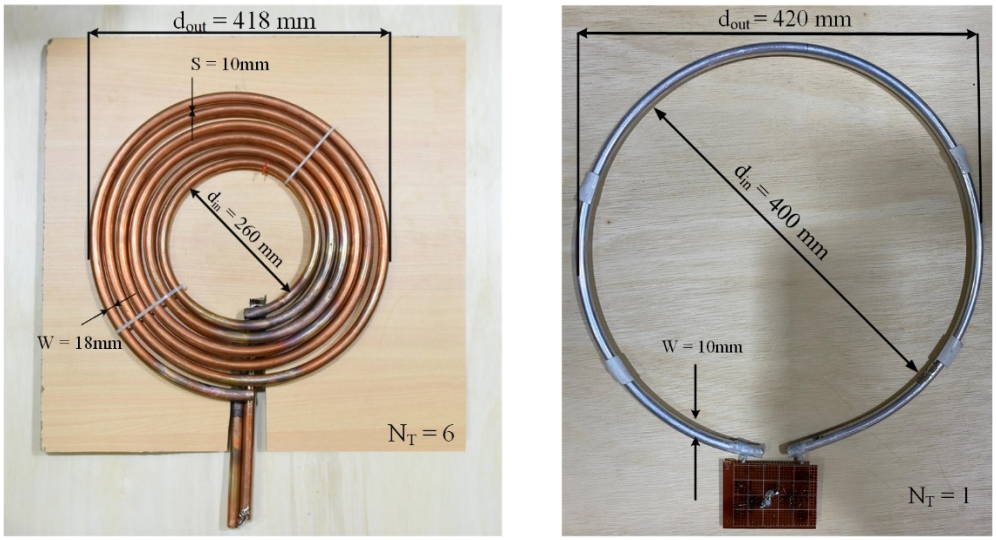

(**a**) (**b**)

Figure 5. Coil design specification for (**a**) transmitter (MTSCC) and (**b**) receiver (STLAC) coils.

Figure 5a,b display the designs of the transmitter and receiver coils with d_{out}, d_{in}, N_T, W, and S.

The implications standard of the present study in Class E PA switching was the use of constant envelope modulation techniques, such that the signal does not carry any amplitude information because of the assertive amplitude compression suffered in PA switching [49]. The transmitter and receiver coil matching network accounts for a great portion of the power loss. A great matching network design between PA and antenna coils is necessary. Therefore, all the power is delivered to the load. Various architectures are available for constructing a power amplifier that converts DC–DC voltage, such as Class E PAs [50]. The efficiency does not represent a physical parameter, it is only helpful for showing the requirements of the circuit for matching and stability. The advantage of Class E PAs is: (1) they have simple architecture and need only one active device; (2) their frequency range is wide KHz–MHz; and (3) they have high power transmission efficiencies. However, the disadvantage of Class E PAs is that any shift in resonance frequency will decrease the output power transmission appreciably. Figure 6 shows the matched resonance frequency

obtained between the transmitter and receiver circuit using the Multisim software for electronic circuit design.

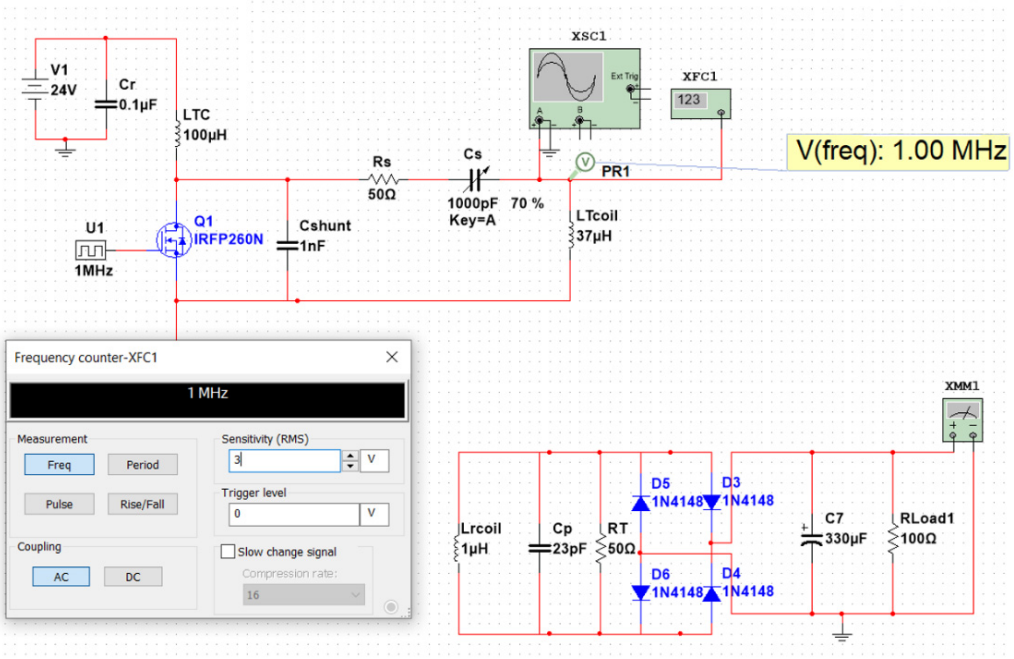

Figure 6. Circuit design using Multisim software to detect the resonance frequency.

The best design from the two configurations (vertical and lateral) was implemented and experimentally tested as MTSCCs and STLACs. The parameters are stated precisely in Tables 1 and 2. The first and second MRC experiments were conducted under loaded conditions. Usually, the resonant wireless power transfer systems require over 1 MHz frequency to get higher efficiency, and it is very complicated to implement such a high frequency because of losses in high frequency alternating current supply. However, lab hardware only allows high-frequency industrial standards to be used, which means the current hardware and tools cannot be upgraded to support higher-frequency industry standards [51,52]. Additional improvements include increasing the frequency to 1 MHz and raising the transfer efficiency. Therefore, 1 MHz is used in the designed model [53]. The usage challenges encountered in the relatively low-frequency range of 1 MHz can be described as follows: (i) reduced transmission efficiency; and (ii) increased size of the transmitter and receiver coils [54].

Table 1. Parameters of Class E PA MTSCC transmitter.

Parameters	Value
Input voltage DC (V/Volt)	24 V
Input current DC (A/Amp)	1.08
Operating frequency (f_0/MHz)	1
Inductance of transmitter choke coil (LTC/µH)	100
Compensating capacitor coil (Cr/µf)	0.1
The capacitor shunt coil (Cshunt/nf)	1
The series capacitor variable resistance (CS/pf)	600
Resistances (Rs/Ω)	50
Inductance of transmitter coil (LTcoil/µH)	37.7

Table 2. Parameters of the STLAC receiver coil.

Parameters	Value
Output voltage DC tests (Volt/Amp)	43.24 V/0.43 A
Operating frequency (f_0/MHz)	1
Resistances (R_T/Ω)	50
Compensating capacitor of receiver coil (CP/pf)	23
Load resistance test (R_L/Ω)	50,100
Inductance of receiver (L_r coil/µH)	1.04
The capacitor filter (C-Filter/µf)	330
M (µH) when k = 0.5 between transmitter and receiver coils	3.10

A substantial enhancement in the coil design of the proposed WPT system is observed by considering the misalignment between the transmitter and the receiver coils. In this study, a Class E PA was used. This enabled (i) a simple architecture with only one active device, (ii) a broad frequency range (kHz–MHz), and (iii) a high power transmission efficiency of 90–95%. For frequency regulation, a series-to-parallel (S–P) topology compensation was chosen. The input circuit consists of an MTSCC transmitter coil connected to an oscillator circuit (i.e., 43.24 V/0.43 A) with a DC input voltage and current (i.e., 24 V/1.08 A) that generates oscillations, where according to some of the tests that have been conducted for building an oscillator circuit, the best transistor type is IRFP510N. The voltage that is available to the input circuit can be increased using three metal-oxide-semiconductor-field-effect transistors (test: IRFP250N, IRFP460LC, and IRFP510N), two parallel coupling capacitors, a capacitor shunt, and one radio-frequency choke coil. The STLAC, four parallel coupling capacitors for testing, a bridge rectifier, a resistance load (100 Ω/50 W) for testing, and a charging controller to charge the drone's battery with a proper voltage (i.e., 24 V) are the primary components of the receiver circuit, as indicated in Tables 1 and 2.

The most significant objective in this test is to find the resonance (matching network) between the transmitter and reception coils by determining the optimal capacitance and resistance values for both coils' inductance values. For the X525 quadcopter drone, this research uses a 22.2 V/5500 mAh Li-Po battery. The drone's battery is charged using the receiving coil. The STLAC and MTSCC parameter requirements are supplied in Table 3, and the measurements and computations are reported in Table 4.

Table 3. Specifications and parameters of the transmitter and receiver coils.

Specification of Coils	MTSCC	STLAC
(Number of turns (N_T)) based on Equation (16)	6	1
Line width (W) (mm)	18	10
Line space (S) for two transmitters (mm)	20	zero
Outer diameter of the coil ((d_{out}/mm)	418	420
Inner diameter of the coil (d_{in}/mm)	260	400

Table 4. The measurements and calculations of the transmitter and receiver coils.

Measurement of Coils	Receiver Coil (STLAC)	Transmitter Coil (MTSCC)
(Inductance (L_S) and (L_R) (µH)) based on Equation (13)	1.04	37.7
(Q_{total}) based on Equations (3) and (4) in simulation (alignment (vertical) at 2 cm of transfer distance)	54	111.49
(Q_{total}) based on Equations (3) and (4) in simulation (lateral misalignment at 2 cm of transfer distance)	109	105
(Q_{total}) based on Equation (18) in measurement	7.43	5.01
Weight (kg)	0.0105	2000

Next, the coil was rounded until the required turns were achieved (Figure 7). The coil's ends were then welded with oxygen welding. However, the coaxial port was welded with a Veroboard to avoid poor conduction. In this study, the ideal coil is considered as having high transfer power and efficiency, while being of suitably low weight as not to hinder flying drone performance. The transmitter coil was made from copper and glued on the pad with a small amount of inlayed plastic around the coil to improve the inductance with the perfect design of spaces between turns.

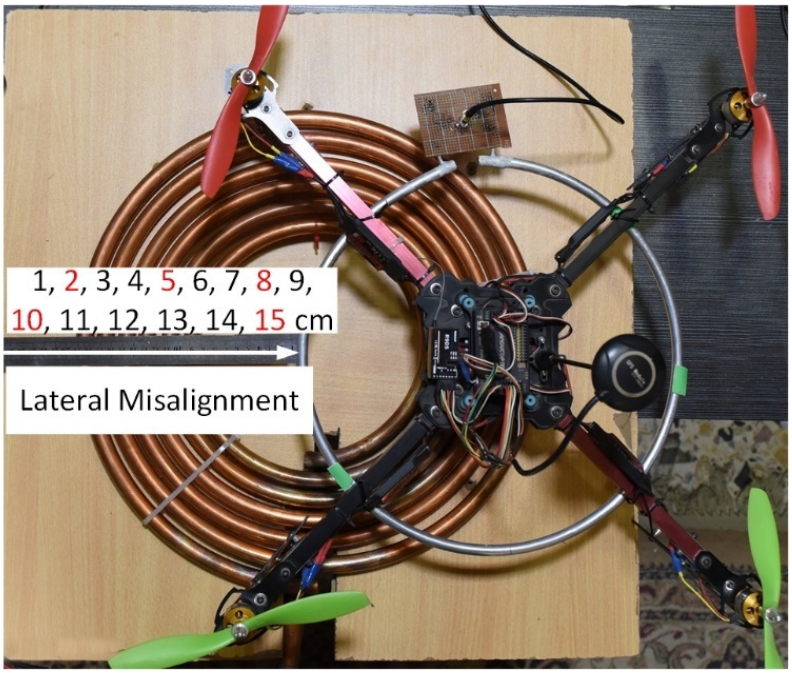

Figure 7. Lateral misalignment distance tests of 2 cm, 5 cm, 8 cm, 10 cm, and 15 cm with the base station pad.

6.1. Alignment and Misalignment Configuration

This work achieved the reduction of the misalignment problem from the lateral configuration by adopting a large primary and secondary coil configuration. The receiver coil was configured as an STLAC with one turn and was employed alongside the receiver circuit with the transmitter coil (i.e., MTSCC). Five different misalignment distance values were selected as 2, 5, 8, 10, and 15 cm (Figure 7: red color), and other distances were almost the same value at 2 cm of the vertical distance between receiver and transmitter coil, which were experimentally tested to evaluate the energy transfer performance. The pad of the base station was implemented to ensure a lateral misalignment of not more than 15 cm between the transmitter and the receiver coils, as shown in Figure 7. The transfer power and efficiency were measured for these distances during drone landing. The direct current (DC) and voltage were measured with 2 cm of air gap fixed in vertical alignment. However, the DC output power and transfer efficiency were calculated when the drone's battery loaded the receiving circuit.

6.2. WPT Experiment Configuration

The test was mounted using a digital multimeter (DT9205, Dowdon, Shenzhen, China), an oscilloscope (MCP Lab Electronics/DQ7042C, Shanghai MCP Corp, Shanghai, China) and a transmitter using a DC power source (Q-5010S, EMIN Group, Yangon, Myanmar). In both the vertical and lateral configuration tests, the MTSCC was constant, whereas the STLAC was varied based on the different sized air gaps. Several air gap steps were adopted in our experiments due to the proposed loaded and unloaded WPT system, wherein the transfer power and efficiency were decreased to a large extent after 15 cm in the

loaded system. For each position, the transfer voltage, current, power, and efficiency were measured with respect to the distance. The measurements were conducted in a laboratory to test the force sensor of the vertical alignment solution, and lateral misalignment distance when the drone landed on the platform stations.

1. First Experiment: This experiment was for a vertical alignment system with a 100 Ω load. In vertical alignment, air gap/transfer distance measurements of 2 to 50 cm were considered. The MTSCC was tested with the second coil consisting of a one-tap (i.e., an STLAC with one turn). The number of turns was selected based on the first and second simulations, wherein a tradeoff between coil weight, transfer power, and efficiency was achieved to obtain an acceptable transfer performance and weight. Figure 8a shows an example of the vertical alignment improvement in transfer distance between 2 cm to 50 cm when R_L = 100 Ω.

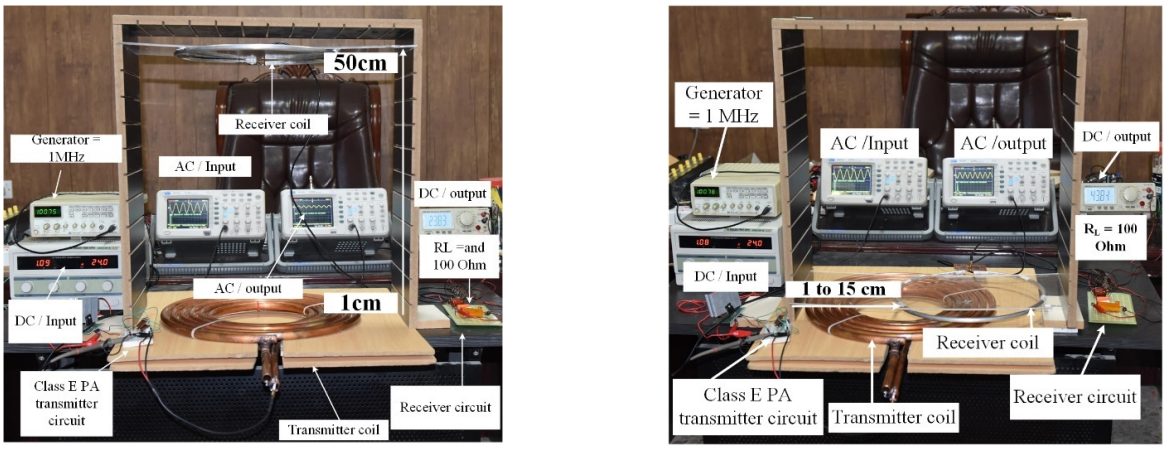

Figure 8. Measurement of the implemented MRC WPT at different distances in the laboratory for: (**a**) vertical alignment with coil drone at 2 and 50 cm at R_L 100 Ω; and (**b**) lateral misalignment in the laboratory at values of 2 cm (vertical) and 15 cm (lateral).

2. Second Experiment: The experiment for a lateral misalignment system with 100 Ω of load, on a pad size of 60 × 60 cm^2. A total of five lateral misalignment distances (selected distance, e.g., 2, 5, 8, 10, and 15 cm) were investigated in this experiment. Figure 8b shows lab measurements for 1 and 15 cm of minimum and maximum lateral misalignment distance range values available in the platform station space.

The payload of the drone also poses a challenge to this design. Consequently, the receiver coil (STLAC) and the breadboard's weight in the receiver circuit were reduced as much as possible to 0.0105 and 0.0015 kg, respectively. The final total weight of the drone was 1.377 kg. The receiver coil only takes up 0.785% (i.e., 0.0105/1.337 × 100%) of the drone's weight, while the total payload (aluminum coil and breadboard with receiver circuit) takes up 0.89% (i.e., 0.012/1.337 × 100%). The measured weights for parts of the drone and coil are listed in Table 5.

Table 5. Calculation of drone weight.

Parameter	Weight in (kg)
The aluminum coil weight (STLAC)	0.0105
A breadboard of the receiver circuit	0.0015
A small piece of wood (200 × 200 mm^2) for the platform station	0.028
Payload weight	0.012
Drone weight	1.337
Ratio of payload weight to the drone weight	0.89%
Ratio of onboard coil weight (aluminum) to the total drone weight	0.785%

6.3. Detection of the Drone on the WPT Circuit

To detect the drone landing in the experiment, a four FSR sensor configuration, which was adapted from [29,38,55] was set up on the squared platform (Figure 9a). The sensors were installed at the edges of the platform using a small spiral spring and 20 × 20 cm^2 of wood (Figure 9b). The wood's weight will be increased when a drone lands. An Arduino UNO and the four FSRs (i.e., Dy1, Dy2, Dx1, and Dx2) were connected to the platform station to start charging when the drone lands. The Arduino functions to read the signal from the FSR, convert the signal to the equivalent weight, and finally reduce the power consumption using the sleep/wakeup strategy. In addition, the regulator and relay circuit required for each voltage, which depends on the drone's weight, can sense the FSR that is needed to charge the drone.

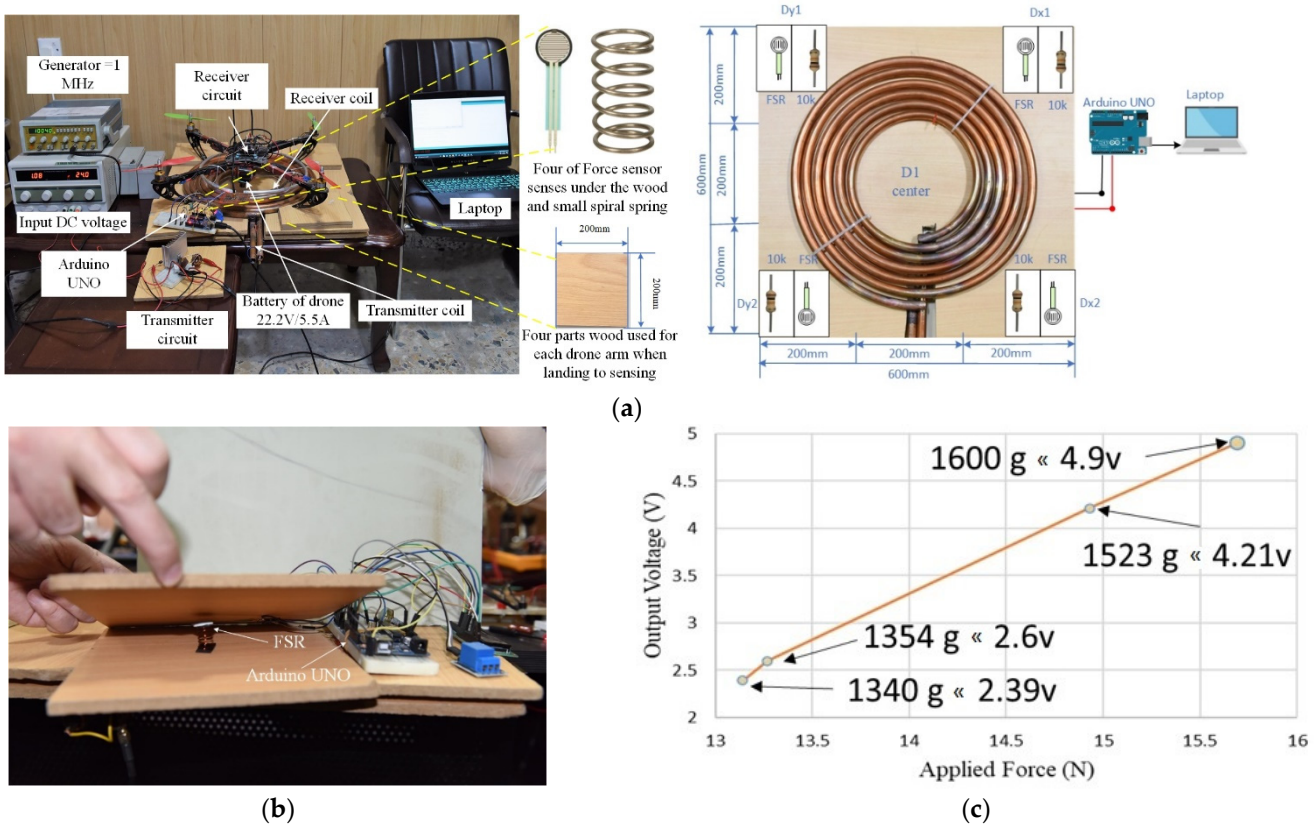

Figure 9. Small-wood testing of the solution with Arduino UNO before the start mission of: (**a**) a platform station using four FSRs; (**b**) FSR connected to Arduino Uno; and (**c**) the calibration of the FSR after drone landing.

The calibration of the FSR before drone landing was tested in the lab, as shown in Figure 9c, and was based on four different drone weights. The four weights (i.e., 1600, 1523, 1354, and 1340 g) were converted to Newton (N) units and are presented on the *x*-axis as the applied force. The *y*-axis presents the output voltage for each sensor's force measurement (4.9, 4.21, 2.6, and 2.39 V).

Figure 10 describes all the possible directions that platform stations may have in lateral misalignment to charge a drone based on WPT. The FSR measures the threshold weight value of the drone (i.e., 1300 g). The first direction (D) is the center of the platform station, where it is in vertical alignment. In addition, the lateral misalignment is represented by the four weights based on direction (i.e., east = 1600 g, west = 1523 g, north = 1354 g, and south = 1340 g), according to the platform size (60 × 60 cm^2) used in this work. The four directions of the different weights measured during the drone landing test conducted in the lab can enable the charging of the drone battery for different durations. However, the

lightweight direction (such as 1340 g) will be the best for charging the drone's battery. The misalignment distance is essential to efficiently determine the weight trend of the drone, as well as the wirelessly transferred power of stationary MRC charging at all power levels according to the FSR technique, which operates by the programming of the four directions into the Arduino UNO. This proposed misalignment algorithm is suitable for any power level designed for drones and can improve transfer efficiency.

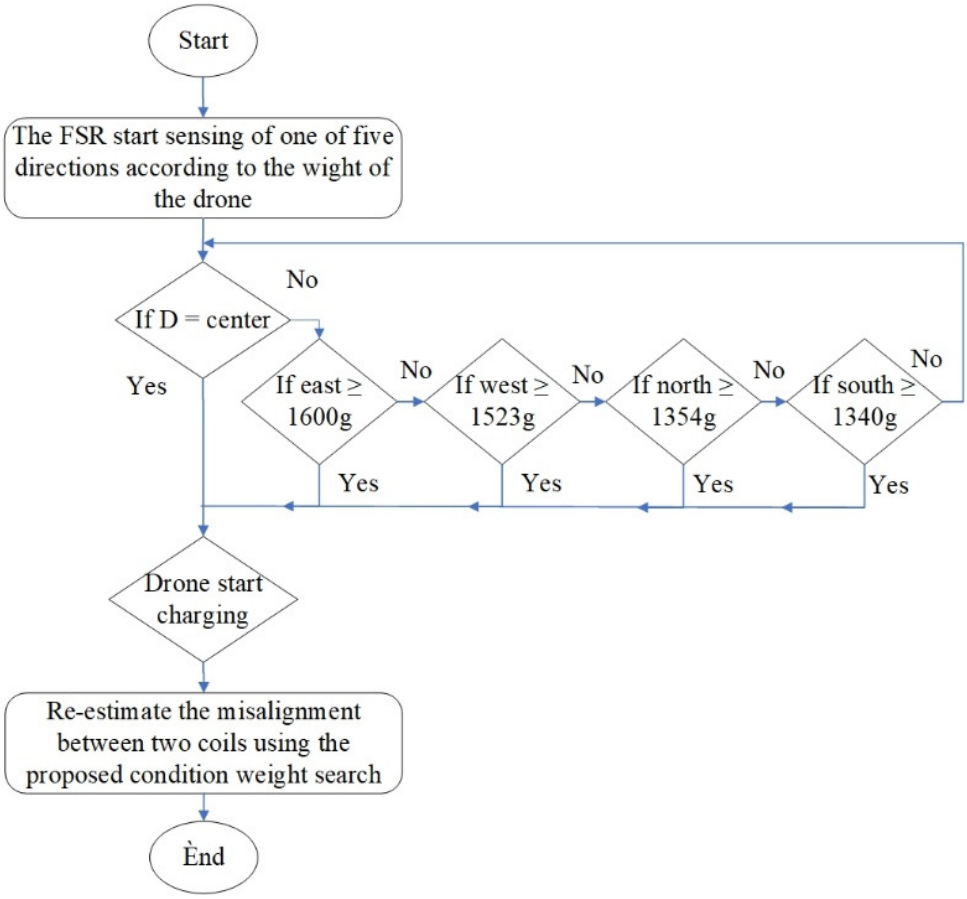

Figure 10. The flowchart of methodology used to solve the different distances and direction of vertical alignment and lateral misalignment.

7. Results

The following subsections present the simulation results, analysis, and discussion of the MTSCC and STLAC designs with related parameters (such as *L*, *M*, *k*, and *Q*), the transfer efficiency link and maximum wireless power efficiency.

7.1. Simulation Results

7.1.1. First Simulation: Vertical Alignment

The transmitter coil's six turns were designed with an 18 mm diameter, while the receiver coil's one turn used a 10 mm diameter for both types of tube coil. The acceptable efficiency results for charging drones were achieved at a maximum distance of 50 cm. The minimum distance was 2 cm when the drone was in the landing position. Figure 11a,b showed the Z-impedance for a 2 cm transfer distance between vertically aligned transmitter and receiver coils at different frequencies.

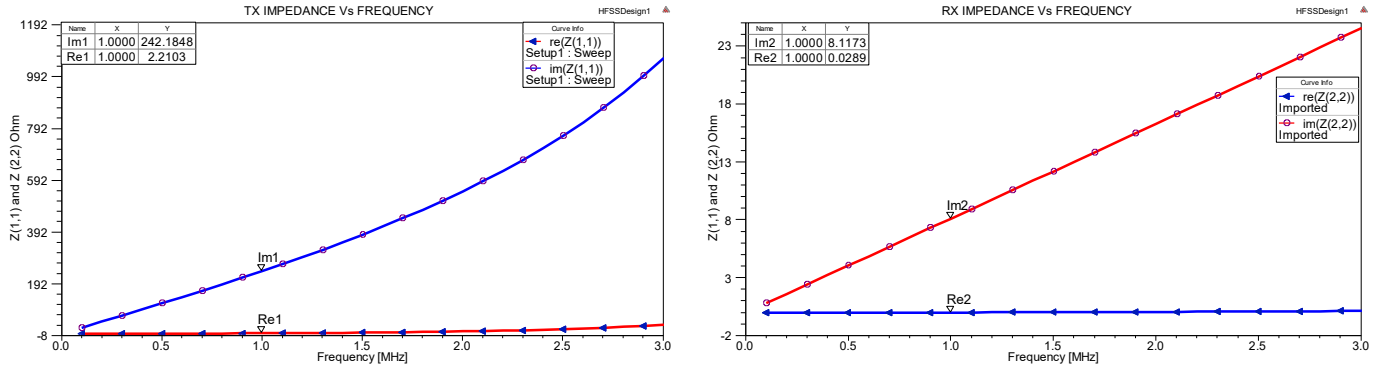

(**a**) (**b**)

Figure 11. The *Im* and *Re* of lumped circuit and performance parameters of vertical alignment at 1 MHz frequency and with a distance equal to 2 cm of Z-impedance: (**a**) Transmitter coil (Tx); and (**b**) receiver coil (Rx).

Figure 12a–c show the Q_1, Q_2, and L_s, L_r, M, and k of the transmitter and receiver coils versus frequency at the maximum transfer distance of 50 cm. Figure 12a, shows the Q_2 (m1: in blue) start to increase when the frequency is equal to 0.125 MHz and the start range decreases from 0.25 to 1.5 MHz because of the proximity to the 2 cm air gap, and the differences in the design of the coils such as the values of N_T, d_{out}, and d_{in} between transmitter and receiver coils. Therefore, the Q_1 (m2: in red) increased slightly from 0.3 to 0.7 MHz before it dropped again. In addition, Figure 12a shows the L_S, L_r (pink and green lines, respectively) values of the transmitter and receiver coils.

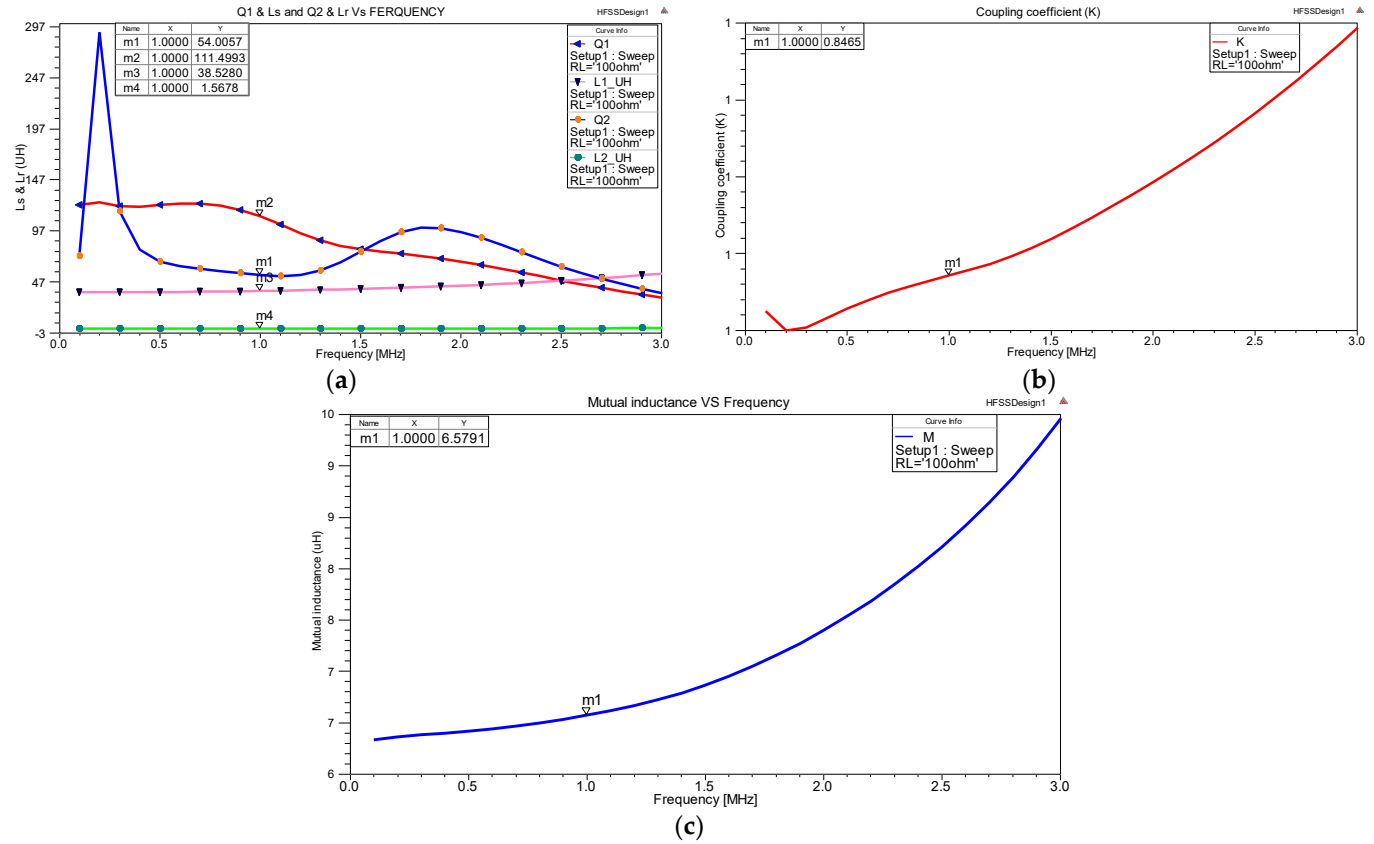

(**a**) (**b**)

(**c**)

Figure 12. The results of the simulation of vertical alignment for 2 cm transfer distance: (**a**) Q_1, Q_2 and L_s, L_r of transmitter and receiver coils, (**b**) k, and (**c**) M of MRC WPT.

Several vertical alignment tests were done with different R_L values (50, 10, 150, 200, 250, 300), and the most suitable value that shows an overall high value between transfer distances from 2 to 50 cm was found when R_L is equal to 100 Ω (cf. Figure 13). To improve the WPT system further, this study investigated the influence of single-core or multi-core tubes on alignment efficiency. The most suitable design was 98% efficient (black line) at 50 mm transfer distance where the Max.WPTE was equal to R_L = 100 Ω. A minimum transfer distance of 2 cm (blue line) is necessary to test the drone, the optimum transfer efficiency (84%) was reached when R_L = 100 Ω, but at Max.WPTE = 97%. At this point, the drone can be recharged when it stops moving.

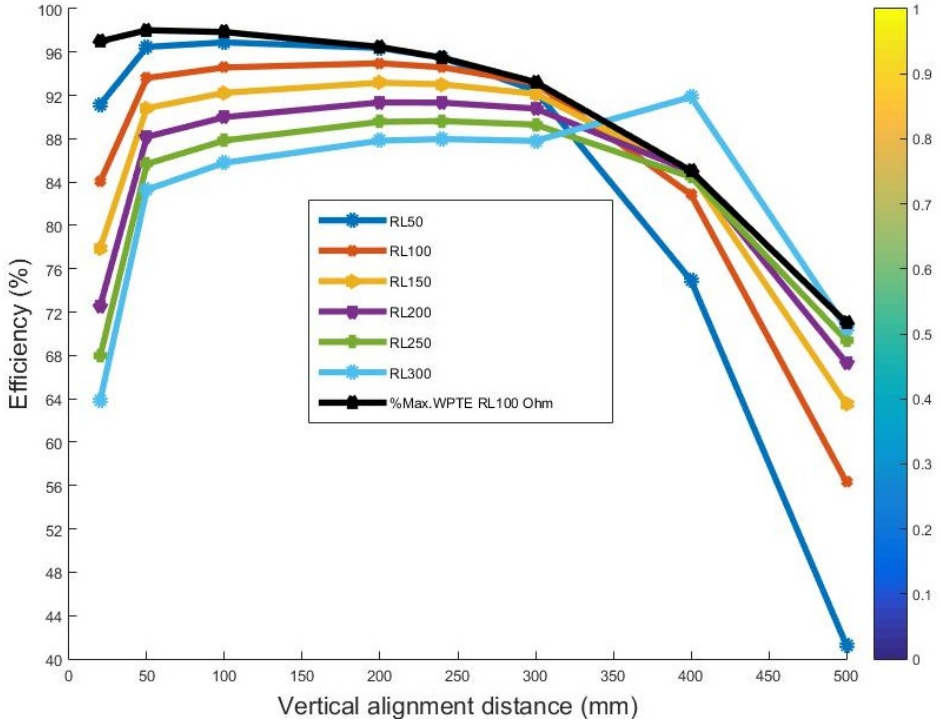

Figure 13. Comparison of different R_L values in simulation of vertical alignment between STLAC and MTSCC lumped parameter performances of efficiency at different R_L values and different distances with Max.WPTE. in mm.

7.1.2. Second Simulation: Lateral Misalignment

Figure 14a,b shows the Z-impedance of *Im* and *Re* at a transfer distance of 2 cm between the transmitter and receiver coils in lateral misalignment.

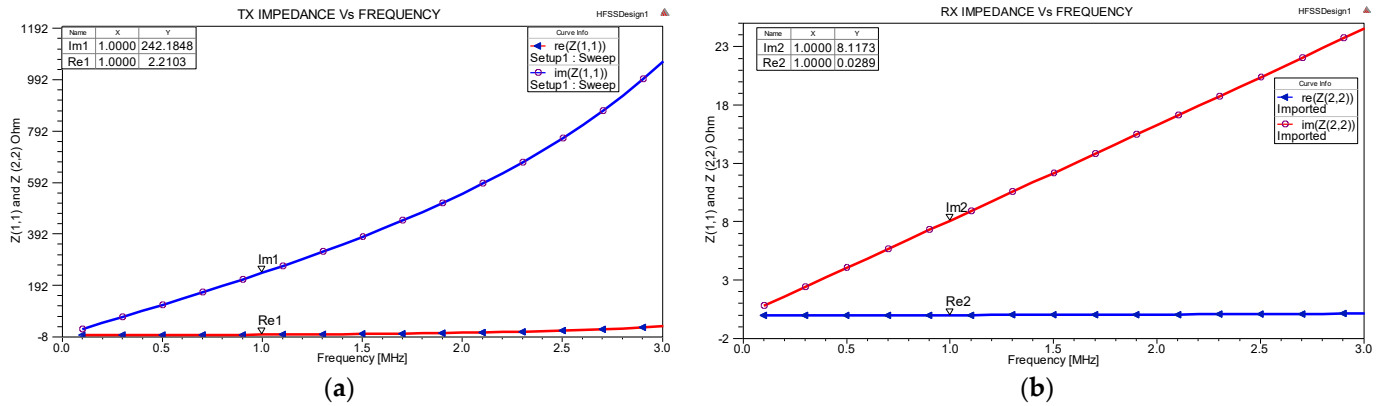

(**a**) (**b**)

Figure 14. The *Im* and *Re* of STLAC and MTSCC lumped circuit and performance parameters of lateral misalignment at a 2 cm distance for (**a**) transmitter coil (T_X), and (**b**) receiver coil (R_X).

Figure 15 shows the results of (Q_{total} = Q_1 and Q_2) M, and k between the transmitter and receiver coils. The efficiency results of the lateral misalignment distance in the range of 2–15 cm were tested in the R_L range of 50 to 300 Ω. The best Max.WPTE value of 97.77% was selected when R_L = 100 Ω and the red line attained lateral and vertical alignment between two coils at 2 cm. Figure 15a shows the results of L_S, L_r (in pink and green line), and *Q-factor* (in red and blue line) values of the transmitter and receiver coils. The *Q-factors* were increased in the low-frequency range from 0.2 to about 0.4 MHz and decreased in frequency. The Q_{total} values crossed at 0.9 MHz. Meanwhile, the *inductance* settles in green and increases in pink. Figure 15b shows that M, and Figure 15c shows that k increased as the frequency increased from 0.50 to 3 MHz.

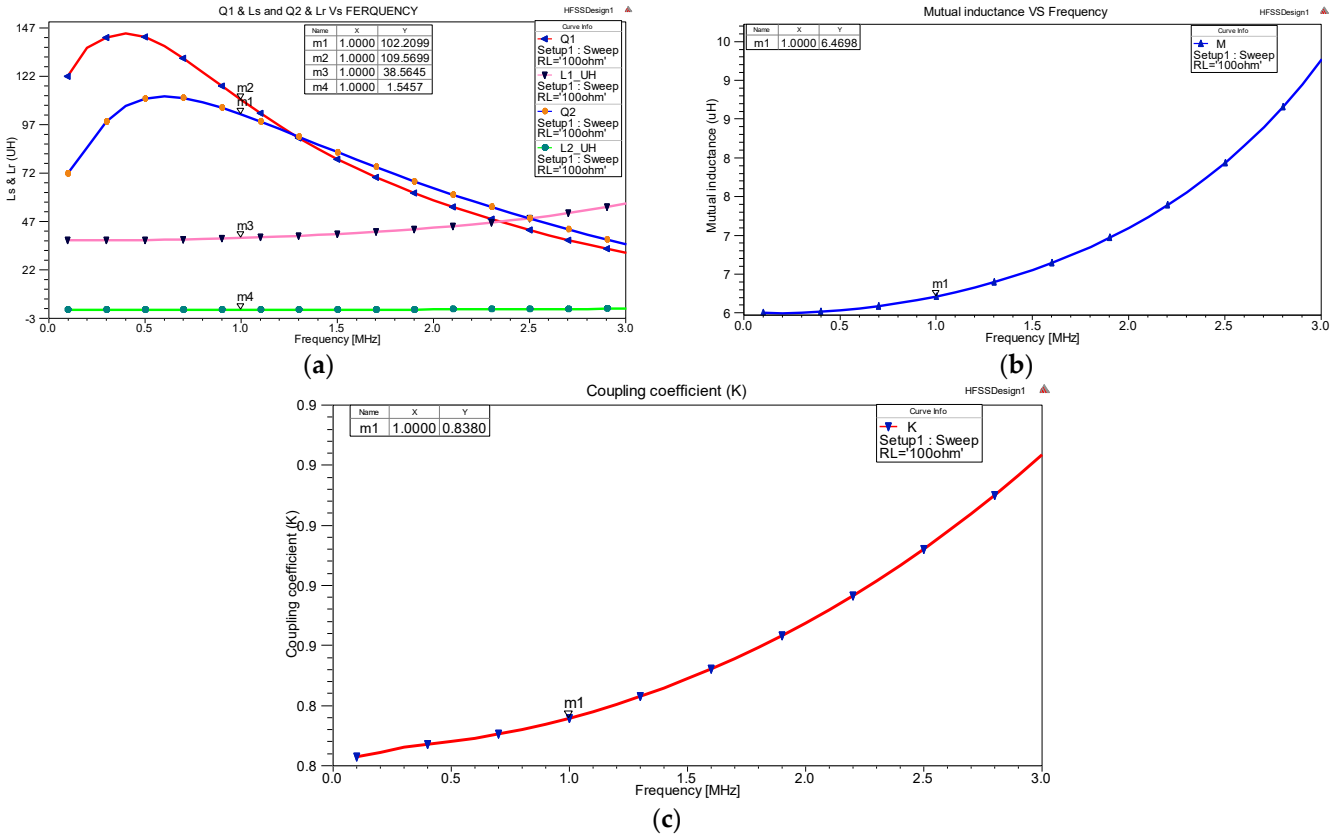

Figure 15. The simulation results of lateral misalignment for 2 cm of transfer distance: (**a**) Q_1, Q_2 and L_S, L_r of transmitter and receiver coils; (**b**) M, and (**c**) k of MRC WPT.

The optimal values of the tested R_L between the simulated coil designs ranged from 50 to 300 Ω and for variation of distance from 20 to 150 mm are shown in Figure 16a. Max.WPTE at R_L equal to 100 Ω and with 15 cm of transfer distance resulted in a 91.44% improvement in transfer efficiency. The lowest efficiency was obtained with R_L = 300 Ω at 150 mm (15 cm) transfer distance. The corresponding optimal number of turns of the transmitter coil of the platform station was calculated with respect to the maximum link efficiency and using different values of load resistance as shown in Figure 16b. It is clear from this figure that the optimal load resistance for this case was when R_L values equaled 50 and 100 Ω, with an efficiency of 96.5%.

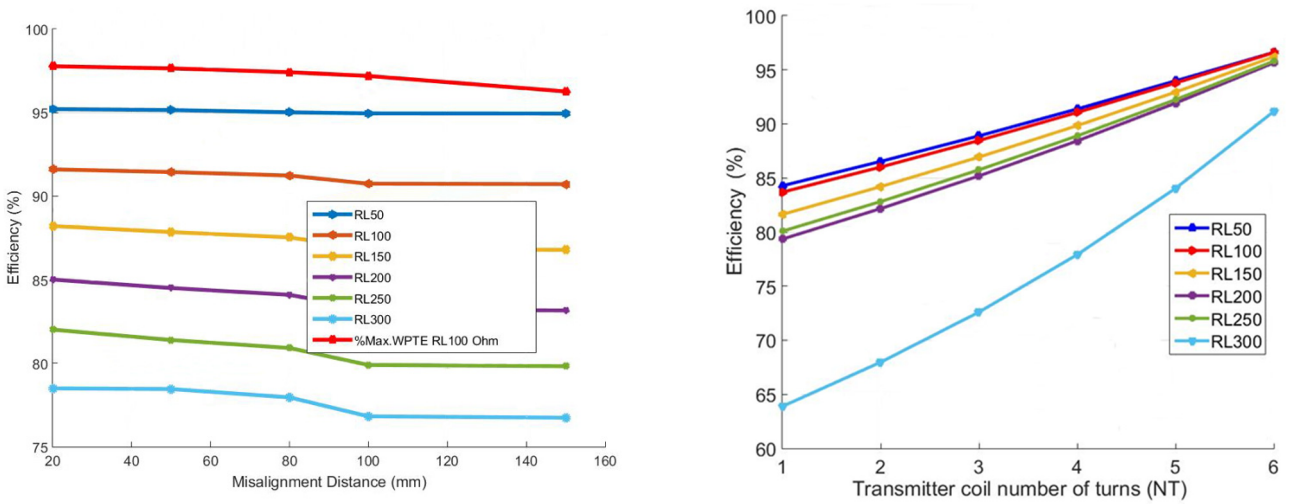

(**a**) (**b**)

Figure 16. Comparison of different R_L values in simulation between STLAC. (**a**) The drone's available distance range was between 2 to 15 cm and MTSCC (fixed) in lateral misalignment for improving transfer efficiency at 20 mm distance; and (**b**) the best selection results of the transmitter of design coil in simulation.

7.2. Experimental Results

WPT was practically implemented based on MTSCC design in the transmitter circuit and STLAC in a receiver (the drone's circuit) to align and misalign configurations at different distances. The following subsections focus on the laboratory results.

7.2.1. First Experiment: Vertical Alignment

The experiment was implemented for the vertical alignment system under a load condition (i.e., drone battery). This number of transmitter coil turns (N_T = 1 to 6) was selected according to the simulation results (Figure 16b) of the first (vertical alignment) and second (lateral misalignment) study on transmitter coils design. A tradeoff was achieved between the coil weight (receiver coil) and the transfer performance (transfer power and efficiency).

The relationships between the transfer distance with the DC output power and the transfer efficiency are shown in Figure 17 (primary *y*-axis). Meanwhile, the relationship between transfer distance and the DC output current is presented on the secondary *y*-axis. The figure shows the performance of the STLAC under the tested distance range of 2–50 cm with a load. The DC output power, transfer efficiency, and output current decreased with distance. The DC output power, output current, and efficiency were 21.12 W, 0.460 A, and 81.5%, respectively, at 2 cm and were sufficient for battery charging according to the E PA class circuit designs. The DC output current, output power, and efficiency decreased to 0.359 A, 12.92 W (Left; *y*-axis), and 49.85% (Right; *y*-axis), respectively, at 40 cm and further decreased to 5.53 W, 0.235 A, and 21.38% at 50 cm. The DC output power, output current, and efficiency gradually decreased with distances beyond 30 cm.

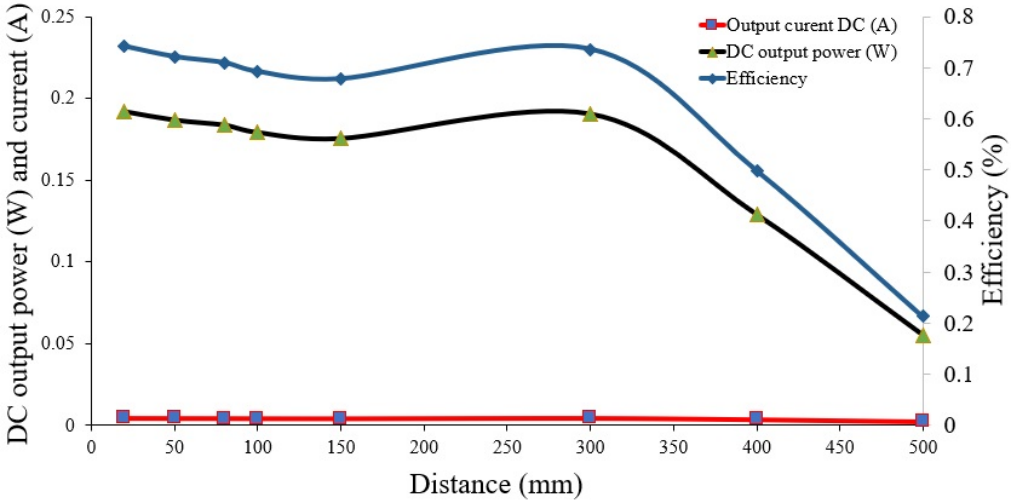

Figure 17. Experimental results of WPT between STLAC, and MTSCC of vertical alignment between transmitter and receiver coils with transfer distance in mm, at R_L 100 Ω of DC output power, and with efficiency and output current measured in A.

7.2.2. Second Experiment: Lateral Misalignment

The MTSCC was first tested with the STLAC using a lightweight coil with one turn under several misalignment situations and under a load condition to explore the amount of transferred DC power and its efficiency. The experiment investigated lateral misalignment between the MTSCC and the STLAC at five distances (2, 5, 8, 10, and 15 cm), and at 2 cm vertical alignment distance.

The maximum transfer output current in the secondary *y*-axis equals 0.438A, while DC power and efficiency equal 19.22 W and 74.15% as shown in the primary *y*-axis, which were recorded at 2 cm lateral misalignment. The transfer DC output power values of 18.70, 17.94, and 17.54 W were noted at 2, 5, and 10 cm lateral misalignments, respectively. The transferred power and efficiency decreased when distance increased for all the lateral misalignments, as shown in Figure 18. Transfer efficiencies of 72.13%, 69.23%, and 67.8% were recorded at 2, 5, and 10 cm lateral misalignment, respectively. The output current decreased with distance for lateral misalignments and vertical distances.

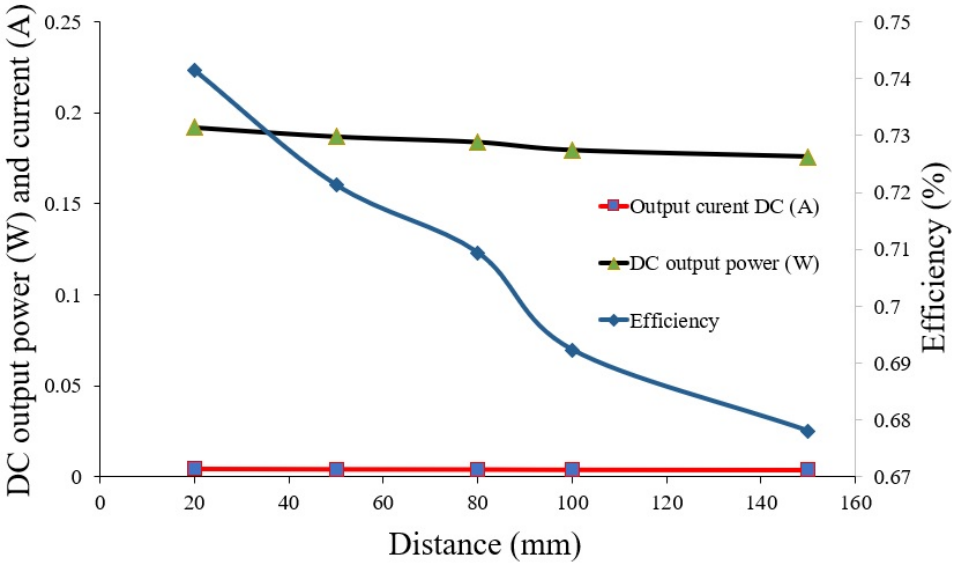

Figure 18. Experimental measurement results of WPT between STLAC and MTSCC in lateral misalignment with DC output power (measured in W), transfer efficiency (%) and output current (measured in A).

7.3. Energy Harvesting Techniques Based on Solar Cell

The current consumption from the battery due to the force sensor is dependent on its application [56]. In this paper, the two solar panels were positioned above the force sensor and microcontroller box. The solar cell angle is oriented toward the sun with an incident angle of 20°–30° relative to the ground [57]. SFPVM-30 type solar cells (KINGRO, Shaoxing, China), which were a first-proposed type of solar cell (36 V/60 W) that deliver a maximum current range of 65,000–200,000 mA, was selected [58]. The measurements and specifications of the solar cell are shown in Table 6.

Table 6. Features of the adopted solar cell.

Parameter	Value
Output voltage	18 V
Load voltage	25 V
Maximum current	1670 mA
Maximum output power (PMAX)	30 W
Dimensions (L × W × T)	445 × 540 × 18 mm^3
Surface area (S)	240.30 cm^2

The battery and solar cells should be created in mathematical models for the force sensor to investigate the harvested energy from the solar cells and battery consumption. The power consumption of the solar cell model of the force sensor, which is based on the battery, is presented in Equations (19) and (20). Solar cell efficiency ($\eta_{Solar\ cell}$) can be calculated as follows [59]:

$$\eta_{Solar\ cell} = P_{MAX}/S_{sa} \times Ra \tag{19}$$

where P_{MAX} is the output power of the solar cell (measured in W), S_{sa} is the surface area of the solar cell (measured in m^2), and Ra is radiation, which is defined as the intensity of the incident light power on the surface of a solar cell (measured in W/m^2). The power of the adopted solar cell can be calculated as in Equation (20).

$$P_{MAX} = V_{solar} \times I_S \tag{20}$$

where V_{solar} is the voltage of the solar cell (measured in Volts) and I_S is the current of the solar cell (measured in mA).

7.4. Analysis and Discussions

The results revealed a maximum power transfer and efficiency of 19.22 W and 74.15%, respectively, for the misalignment condition, and an air gap of 15 cm with a vertical misalignment of 2 cm between two coils under load. However, the MTSCC and STLAC improved power transfer and efficiency to 21.12 W and 81.5%, respectively, at 10 cm. The transmitter and receiver coils could not touch when the system was loaded under the alignment and misalignment conditions. It caused a short circuit between the transmitter and receiver coils when simulated and tested in the laboratory.

The key contributions of this study can be summarized as follows:

1. The application of a high power charging capability circuit design using a Class E PA for the potential deployment of drones in high-power electronic applications like radiation monitoring and smart agriculture. This work extends our previous study [60], where the design was more suitable to lower power consumption applications such as agricultural sensors.
2. A new platform design for near-field WPT based on MRC techniques using the series-to-parallel compensation capacitor topology to improve the power consumption and enhance transfer distance under correct alignment and lateral misalignment cases. The platform is complemented with FSR to identify the orientation of a landed drone based on identifying the weight that suggests the position, such as the western, eastern,

northern, and southern faces of the drone charging platform when in landing/idling modes of operation.

3. Improvement on the misalignment condition between the transmitter and receiver coils for the improved air gap, transfer power efficiency, and payload of drones. The improvement considered the design, simulation, and hardware development of an MTSCC in the transmitter circuit located at the drone charging station and an STLAC in the receiver circuit. Additionally, a comparison of the aluminum coil with the copper coil as the WPT receiver on the drone was performed.

The NF-WPT adopted in this work using an MTSCC and STLAC was compared against previous works, as shown in Table 7. The previous methods were similar to the current work in that they utilized tube coil in the coil design and Class E PAs. The proposed MTSCC (transmitter) and STLAC (receiver) methods differed in terms of the coils' designs and number of turns as both affect the transfer efficiency and transfer distance. The simulation design can increase the transfer efficiency and transfer distance but achieving better efficiency is a function of the design topology, the diameter of the coil, the number of turns, materials used, and load conditions. In addition, the existing literature only improved the transfer efficiency in experimental works, but in this work, the designs were first simulated before being implemented in the hardware. This improved the performance of the designs in this study compared to those found in the existing literature. The comparison of the coils method for WPT and its achieved performance metrics, such as transfer efficiency and distance, type of coil, number of turns, and the applications for vertical alignment and lateral misalignment systems from previous studies, are shown in Table 7.

Table 7. Comparison between the proposed coils method at various vertical alignment and lateral misalignment conditions with previous studies.

Ref	Number of Turns (N_T)		Type of Coil	Type of Misalignment	Transfer Distance (cm)	Transfer Efficiency (%)	Applications
	Tx	Rx					
Kang et al. [29]	5	1	Tube coil	Vertical & Horizontal	0.5	45 for Horizontal and 52 for Vertical	Laptop
Campi et al. [25]	10	1	Litz and aluminum pipe	Vertical	20	89	drone
Lan et al. [26]	2	1	Pipe air-core coils	Horizontal	25	70	Drone (DJI Matrice 100)
This work	6 (MTSCC)	1 (STLAC)	Tube or Pipe (Copper for the transmitter and aluminum for the receiver)	Vertical	2–50	81.5@100 mm, and 78.17@200 mm, 74.15@20 mm, 72.13@50 mm, 70.94@80 mm, 69.23@100 mm, and 67.80@150 mm	Qud. DJI X525 (drone)
This work	6 (MTSCC)	1 (STLAC)		Horizontal	2, 5, 8, 10, and 15		

8. Conclusions and Future Works

This study has designed and implemented an MRC-based solution for a near field wireless power transmission (WPT) drone charging station for remote and unmanned applications, such as radiation monitoring and smart agriculture. The MRC design was distinguished by combining the use of an STLAC on the receiver/drone with an MTSCC on the charging/receiving platform to address transfer power optimization and increased efficiency issues. Several coil designs were assessed in the simulation phase to identify the suitable range of drone position misalignment due to the air gap in wireless charging.

For the simulation, the Class E PA model was designed to test misalignment coils and simulation results were obtained using HFSS 15.03 software. The design resulted in the improvement of vertical alignment transfer power. The results were validated mathematically and in a simulation to demonstrate a tailored MTSCC design with an improved *Q-factor*. The transfer efficiency was 94.58% with a 2 cm air gap distance. The lateral misalignment performed at 94.95% transfer efficiency at values of 2 cm.

When referring to the WPT battery charging system, the coils are usually not aligned, limiting the potential of WPT for future remote applications. The results show that transfer efficiency differs between simulation and measurement for vertical alignment by around 13.08%, and lateral misalignment differs by around 20.8%.

Based on simulation and experiments, a number of six turns in the coil (MTSCC) was selected for a new spiral coil in the transmitter circuit to improve transfer distance and efficiency in relation to lateral misalignment. In practice, STLAC was selected for payload improvement purposes. It also provides the maximum transfer power, efficiency, and range from the source of electricity to the coil in the drone, while also being lightweight.

The misalignment condition is vital for drone charging if they are to be implemented for energy-efficient radiation monitoring and internet of farming technology applictions. Future experiments could use a higher operating frequency in the transmitter circuit to reduce the coil size, *NT*, and weight of the receiver coil mounted on the drone. This has the effect of increased transfer efficiency and output power, and reducing distance in WPT. Additionally, MRC-based WPT requires additional studies to enhance the design of the resonators for large-distance transfers and maximum power transfers during angular and planar charging that will reduce losses in the system.

This study focuses on vertical alignment and lateral misalignment cases. The other two types of drone misalignments (i.e., angular and planar position) are not considered in this work due to hardware limitations. In addition, the results were proposed in sunny weather (summer season in my country) to improve the conditions for solar cell electricity generation, and to maximise transfer power.

However, it is worth investigating the extent to which a single tube in the receiver and multi-tube coils can affect system efficiency in the transmitter coil as part of future work. Additionally, the thickness of the tube coil can affect transfer efficiency when the frequency is 1 MHz. Two materials were investigated and the impact of the number of turns and thickness of the receiver coils were analyzed. However, the most important aspects were: the low weight of the receiver coil (0.0105 kg); and the harmonizing of the inductance and capacitance of the transmitter coil to make a matching circuit between the two coils.

In addition, MRC can be used for mid-range applications (e.g., charging the WSN or UAV) with suitable transfer distances and transfer efficiencies. However, the flight time of the UAV is restricted because of the limited battery capacity. Therefore, the MRC-based WPT offers a good solution to charge the drone battery. Thus, the flight time of the drone can be improved using the STLAC (receiver coil) and MTSCC (transmitter coil), whereas the transmitter coil was designed according to the simulation to increase the transfer power and efficiency while charging the drone battery; the receiver coil was designed in the lab to overcome a heavy payload.

Finally, the *k* and *Q-factor* of the adopted STLAC can be modified, for example, by using a different coil diameter, increasing, or decreasing the N_T, or using a cover shield between the transmitter and receiver to charge the battery for certain applications, such as drones and cell phones, efficiently. Thus, the battery lifetime of the drone can be increased. Furthermore, the designed coil could be chosen by considering the limitations of the coils to improve the performance metrics.

Author Contributions: Conceptualization, R.N. and A.M.J.; methodology, A.M.J. and H.M.J.; formal analysis, R.N., A.M.J., S.K.G., A.A.-S. and N.F.A.; investigation, A.M.J., M.J.A.-A. and N.F.A.; resources, R.N. and S.K.G.; data curation, A.M.J., A.A.-S. and N.F.A.; writing—original draft preparation, A.M.J., H.M.J. and S.K.G.; writing—review and editing, R.N., M.J.A.-A., A.A.-S. and N.F.A.; visualization, A.M.J. and H.M.J.; supervision, R.N., S.K.G. and N.F.A.; project administration, R.N.; funding acquisition, R.N. All authors have read and agreed to the published version of the manuscript.

Funding: We acknowledge the financial support from CRIM, Universiti Kebangsaan Malaysia, under the Dana Impak Perdana (DIP) research fund, with reference number: DIP-2019-014 for the open access fee payment and financial support for related research activities.

Institutional Review Board Statement: Not applicable.

Informed Consent Statement: Not applicable.

Data Availability Statement: Not applicable.

Acknowledgments: We acknowledge the financial support from Universiti Kebangsaan Malaysia, under the grant Dana Impak Perdana (DIP), with reference number: DIP-2019-014.

Conflicts of Interest: The authors declare no conflict of interest.

References

1. Chittoor, P.K.; Chokkalingam, B.; Mihet-Popa, L. A Review on UAV Wireless Charging: Fundamentals, Applications, Charging Techniques and Standards. *IEEE Access* **2021**, *9*, 69235–69266. [CrossRef]
2. Nguyen, M.T.; Nguyen, T.H. Wireless Power Transfer: A survey of techniques, and applications on communication networks. *ICSES Trans. Comput. Netw. Commun.* **2018**, *4*, 1–5.
3. Tan, L.; Zhang, M.; Wang, S.; Pan, S.; Zhang, Z.; Li, J.; Huang, X. The design and optimization of a wireless power transfer system allowing random access for multiple loads. *Energies* **2019**, *12*, 1017. [CrossRef]
4. Lu, M.; Bagheri, M.; James, A.P.; Phung, T. Wireless charging techniques for UAVs: A review, reconceptualization, and extension. *IEEE Access* **2018**, *6*, 29865–29884. [CrossRef]
5. Rao, T.C.; Geetha, K. Categories, standards and recent trends in wireless power transfer: A survey. *Indian J. Sci. Technol.* **2016**, *9*, 20.
6. Wagih, M.; Komolafe, A.; Zaghari, B. Separation-Independent Wearable 6.78 MHz Near-Field Radiative Wireless Power Transfer using Electrically Small Embroidered Textile Coils. *Energies* **2020**, *13*, 528. [CrossRef]
7. Junaid, A.B.; Konoiko, A.; Zweiri, Y.; Sahinkaya, M.N.; Seneviratne, L. Autonomous wireless self-charging for multi-rotor unmanned aerial vehicles. *Energies* **2017**, *10*, 803. [CrossRef]
8. Le, A.; Truong, L.; Quyen, T.; Nguyen, C.; Nguyen, M. Wireless power transfer near-field technologies for unmanned aerial vehicles (uavs): A review. *EAI Endorsed Trans. Ind. Netw. Intell. Syst.* **2020**, *7*, 162831. [CrossRef]
9. Campi, T.; Cruciani, S.; Feliziani, M. Wireless power transfer technology applied to an autonomous electric UAV with a small secondary coil. *Energies* **2018**, *11*, 352. [CrossRef]
10. Joy, E.R.; Dalal, A.; Kumar, P. Accurate computation of mutual inductance of two air core square coils with lateral and angular misalignments in a flat planar surface. *IEEE Trans. Magn.* **2013**, *50*, 1–9. [CrossRef]
11. Huang, W.; Ku, H. Analysis and optimization of wireless power transfer efficiency considering the tilt angle of a coil. *J. Electromagn. Eng. Sci.* **2018**, *18*, 13–19. [CrossRef]
12. Patil, D.; Ditsworth, M.; Pacheco, J.; Cai, W. A magnetically enhanced wireless power transfer system for compensation of misalignment in mobile charging platforms. In Proceedings of the 2015 IEEE Energy Conversion Congress and Exposition (ECCE), Montreal, QC, Canada, 20–24 September 2015; pp. 1286–1293.
13. Zhong, W.; Liu, X.; Hui, S.R. A novel single-layer winding array and receiver coil structure for contactless battery charging systems with free-positioning and localized charging features. *IEEE Trans. Ind. Electron.* **2010**, *58*, 4136–4144. [CrossRef]
14. Eteng, A.A.; Rahim, S.K.A.; Leow, C.Y.; Jayaprakasam, S.; Chew, B.W. Low-power near-field magnetic wireless energy transfer links: A review of architectures and design approaches. *Renew. Sustain. Energy Rev.* **2017**, *77*, 486–505. [CrossRef]
15. Simic, M.; Bil, C.; Vojisavljevic, V. Investigation in wireless power transmission for UAV charging. *Procedia Comput. Sci.* **2015**, *60*, 1846–1855. [CrossRef]
16. Chhawchharia, S.; Sahoo, S.K.; Balamurugan, M.; Sukchai, S.; Yanine, F. Investigation of wireless power transfer applications with a focus on renewable energy. *Renew. Sustain. Energy Rev.* **2018**, *91*, 888–902. [CrossRef]
17. Li, J.; Yin, F.; Wang, L.; Cui, B.; Yang, D. Electromagnetic induction position sensor applied to anti-misalignment wireless charging for uavs. *IEEE Sens. J.* **2019**, *20*, 515–524. [CrossRef]
18. Ni, W.; Collings, I.B.; Wang, X.; Liu, R.P.; Kajan, A.; Hedley, M.; Abolhasan, M. Radio alignment for inductive charging of electric vehicles. *IEEE Trans. Ind. Inform.* **2015**, *11*, 427–440. [CrossRef]
19. Kim, J.; Son, H.-C.; Park, Y.-J. Multi-loop coil supporting uniform mutual inductances for free-positioning WPT. *Electron. Lett.* **2013**, *49*, 417–419. [CrossRef]
20. Fotopoulou, K.; Flynn, B.W. Wireless power transfer in loosely coupled links: Coil misalignment model. *IEEE Trans. Magn.* **2010**, *47*, 416–430. [CrossRef]
21. Dang, Z.; Qahouq, J.A.A. Range and misalignment tolerance comparisons between two-coil and four-coil wireless power transfer systems. In Proceedings of the 2015 IEEE Applied Power Electron. Conference and Exposition (APEC), Charlotte, NC, USA, 15–19 March 2015; pp. 1234–1240.
22. Xie, L.; Shi, Y.; Hou, Y.T.; Lou, A. Wireless power transfer and applications to sensor networks. *IEEE Wirel. Commun.* **2013**, *20*, 140–145.
23. Niu, W.-Q.; Chu, J.-X.; Gu, W.; Shen, A.-D. Exact analysis of frequency splitting phenomena of contactless power transfer systems. *IEEE Trans. Circuits Syst. I Regul. Pap.* **2012**, *60*, 1670–1677. [CrossRef]
24. Abou Houran, M.; Yang, X.; Chen, W. Magnetically coupled resonance WPT: Review of compensation topologies, resonator structures with misalignment, and EMI diagnostics. *Electronics* **2018**, *7*, 296. [CrossRef]

25. Campi, T.; Cruciani, S.; Maradei, F.; Feliziani, M. Wireless charging system integrated in a small unmanned aerial vehicle (UAV) with high tolerance to planar coil misalignment. In Proceedings of the 2019 Joint International Symposium on Electromagnetic Compatibility, Sapporo and Asia-Pacific International Symposium on Electromagnetic Compatibility (EMC Sapporo/APEMC), Sapporo, Japan, 3–7 June 2019; pp. 601–604.
26. Lan, L.; Kwan, C.H.; Arteaga, J.M.; Yates, D.C.; Mitcheson, P.D. A 100W 6.78 MHz Inductive Power Transfer System for Drones. In Proceedings of the 2020 14th European Conference on Antennas and Propagation (EuCAP), Copenhagen, Denmark, 15–20 March 2020; pp. 1–4.
27. Yusmarnita, Y.; Saat, S.; Hamidon, A.; Husin, H.; Jamal, N.; Kh, K.; Hindustan, I. Design and analysis of 1MHz class-E power amplifier. *WSEAS Trans. Circuits Syst.* **2015**, *14*, 372–378.
28. Wang, Y.; Song, J.; Lin, L.; Wu, X. Parameters calculation and simulation of magnetic coupling resonance wireless power transfer system. In Proceedings of the 2016 Asia-Pacific International Symposium on Electromagnetic Compatibility (APEMC), Shenzhen, China, 17–21 May 2016; pp. 587–590.
29. Kang, S.H.; Jung, C.W. Transfer efficiency of a misalignment of resonators in MR-WPT for a laptop computer with SGR. *Microw. Opt. Technol. Lett.* **2017**, *59*, 2016–2021. [CrossRef]
30. Rybicki, K.; Wojciechowski, R.M. Analysis and design of a class E current-driven rectifier for 1 MHz wireless power transfer system. *J. Electr. Eng.* **2019**, *70*, 58–63. [CrossRef]
31. Kushwaha, B.K.; Rituraj, G.; Kumar, P. 3-D analytical model for computation of mutual inductance for different misalignments with shielding in wireless power transfer system. *IEEE Trans. Trans. Electrif.* **2017**, *3*, 332–342. [CrossRef]
32. Varghese, B.J.; Bobba, P.B.; Kavitha, M. Effects of coil misalignment in a four coil implantable wireless power transfer system. In Proceedings of the 2016 IEEE 7th Power India International Conference (PIICON), Bikaner, India, 25–27 November 2016; pp. 1–6.
33. Rohan, A.; Rabah, M.; Asghar, F.; Talha, M.; Kim, S.-H. Advanced drone battery charging system. *J. Electr. Eng. Technol.* **2019**, *14*, 1395–1405. [CrossRef]
34. Kim, J.; Jeong, J. Range-adaptive wireless power transfer using multiloop and tunable matching techniques. *IEEE Trans. Ind. Electron.* **2015**, *62*, 6233–6241. [CrossRef]
35. Ahmad, A.; Alam, M.S.; Varshney, Y.; Khan, R.H. A state of the Art review on Wireless Power Transfer a step towards sustainable mobility. In Proceedings of the 2017 14th IEEE India Council International Conference (INDICON), Roorkee, India, 15–17 December 2017; pp. 1–6.
36. Arteaga, J.M.; Aldhaher, S.; Kkelis, G.; Yates, D.C.; Mitcheson, P.D. Multi-MHz IPT systems for variable coupling. *IEEE Trans. Power Electron.* **2017**, *33*, 7744–7758. [CrossRef]
37. Wu, W.; Fang, Q. Design and simulation of printed spiral coil used in wireless power transmission systems for implant medical devices. In Proceedings of the 2011 Annual International Conference of the IEEE Engineering in Medicine and Biology Society, Boston, MA, USA, 3 September 2011; pp. 4018–4021.
38. Olivo, J.; Carrara, S.; De Micheli, G. A study of multi-layer spiral inductors for remote powering of implantable sensors. *IEEE Trans. Biomed. Circuits Syst.* **2013**, *7*, 536–547. [CrossRef]
39. Raju, S.; Prawoto, C.C.; Chan, M.; Yue, C.P. Modeling of on-chip wireless power transmission system. In Proceedings of the 2015 IEEE International Wireless Symposium (IWS 2015), Shenzhen, China, 30 March–1 April 2015; pp. 1–4.
40. Jun, B.O.; Kim, H.J.; Heo, S.J.; Kim, J.; Yang, J.H.; Kim, S.; Kim, K.; Jin, W.C.; Choi, J.W.; Jang, J.E. Miniaturized Self-Resonant Micro Coil Array with A Floating Structure for Wireless Multi-Channel Transmission. *Adv. Sci.* **2021**, *8*, 2102944. [CrossRef] [PubMed]
41. Mehri, S.; Ammari, A.C.; Ben Hadj Slama, J.; Rmili, H. Geometry optimization approaches of inductively coupled printed spiral coils for remote powering of implantable biomedical sensors. *J. Sens.* **2016**, *2016*, 1–11. [CrossRef]
42. RamRakhyani, A.K.; Mirabbasi, S.; Chiao, M. Design and optimization of resonance-based efficient wireless power delivery systems for biomedical implants. *IEEE Trans. Biomed. Circuits Syst.* **2010**, *5*, 48–63. [CrossRef] [PubMed]
43. Yue, C.P.; Wong, S.S. Physical modeling of spiral inductors on silicon. *IEEE Trans. Electron Devices* **2000**, *47*, 560–568. [CrossRef]
44. Tesla, N. *The Strange Life of Nikola Tesla*; Library of Alexandria: Alexandria, Egypt, 2020; Volume 1.
45. Cai, C.; Wang, J.; Nie, H.; Zhang, P.; Lin, Z.; Zhou, Y.-G. Effective-Configuration WPT Systems for Drones Charging Area Extension Featuring Quasi-Uniform Magnetic Coupling. *IEEE Trans. Trans. Electrif.* **2020**, *6*, 920–934. [CrossRef]
46. Choi, B.H.; Thai, V.X.; Lee, E.S.; Kim, J.H.; Rim, C.T. Dipole-coil-based wide-range inductive power transfer systems for wireless sensors. *IEEE Trans. Ind. Electron.* **2016**, *63*, 3158–3167. [CrossRef]
47. Park, C.; Lee, S.; Cho, G.-H.; Rim, C.T. Innovative 5-m-off-distance inductive power transfer systems with optimally shaped dipole coils. *IEEE Trans. Power Electron.* **2015**, *30*, 817–827. [CrossRef]
48. ANSYS HFSS v15.03 Software. Available online: http://www.Ansys.com/products/electronics/ansys-hfss (accessed on 3 August 2021).
49. Mutashar, S.; Hannan, M.; Samad, S.A.; Hussain, A. Development of bio-implanted micro-system with self-recovery ask demodulator for transcutaneous applications. *J. Mech. Med. Biol.* **2014**, *14*, 1450062. [CrossRef]
50. Hannan, M.A.; Hussein, H.A.; Mutashar, S.; Samad, S.A.; Hussain, A. Automatic frequency controller for power amplifiers used in bio-implanted applications: Issues and challenges. *Sensors* **2014**, *14*, 23843–23870. [CrossRef]
51. Jadidian, J.; Katabi, D. Magnetic MIMO: How to charge your phone in your pocket. In Proceedings of the 20th Annual International Conference on Mobile Computing and Networking, Maui Hawaii, HI, USA, 7–11 September 2014; pp. 495–506.

52. Shi, L.; Kabelac, Z.; Katabi, D.; Perreault, D. Wireless power hotspot that charges all of your devices. In Proceedings of the 21st Annual International Conference on Mobile Computing and Networking, Paris, France, 10 September 2015; pp. 2–13.
53. Rehman, M.; Baharudin, Z.; Nallagownden, P.; Islam, B.; Rehman, M.U. Modeling and analysis of series-series and series-parallel combined topology for wireless power transfer using Multiple coupling coefficients. *IJCSNS* **2017**, *17*, 114.
54. Jiang, H.; Zhang, J.; Lan, D.; Chao, K.K.; Liou, S.; Shahnasser, H.; Fechter, R.; Hirose, S.; Harrison, M.; Roy, S. A low-frequency versatile wireless power transfer technology for biomedical implants. *IEEE Trans. Biomed. Circuits Syst.* **2012**, *7*, 526–535. [CrossRef] [PubMed]
55. Cheon, D.-h.; Choi, J.-w.; Lee, J.-m. 4-leg landing platform with sensing for reliable rough landing of multi-copters. In Proceedings of the International Conference on Intelligent Robotics and Applications, Yantai, China, 9 January 2021; pp. 364–373.
56. Escolar, S.; Chessa, S.; Carretero, J. Energy management in solar cells powered wireless sensor networks for quality of service optimization. *Pers. Ubiquitous Comput.* **2014**, *18*, 449–464. [CrossRef]
57. Mesas-Carrascosa, F.; Santano, D.V.; Meroño, J.; De La Orden, M.S.; García-Ferrer, A. Open source hardware to monitor environmental parameters in precision agriculture. *Biosyst. Eng.* **2015**, *137*, 73–83. [CrossRef]
58. Wang, C.; Ma, Z. Design of wireless power transfer device for UAV. In Proceedings of the 2016 IEEE International Conference on Mechatronics and Automation, Harbin, China, 7–10 August 2016; pp. 2449–2454.
59. Zou, T.; Lin, S.; Feng, Q.; Chen, Y. Energy-efficient control with harvesting predictions for solar-powered wireless sensor networks. *Sensors* **2016**, *16*, 53. [CrossRef] [PubMed]
60. Jawad, A.M.; Jawad, H.M.; Nordin, R.; Gharghan, S.K.; Abdullah, N.F.; Abu-Alshaeer, M.J. Wireless power transfer with magnetic resonator coupling and sleep/active strategy for a drone charging station in smart agriculture. *IEEE Access* **2019**, *7*, 139839–139851. [CrossRef]